UCRL-16443

University of California

Ernest O. Lawrence Radiation Laboratory

DECAY PROPERTIES OF THE ω MESON

TWO-WEEK LOAN COPY

This is a Library Circulating Copy which may be borrowed for two weeks. For a personal retention copy, call Tech. Info. Division, Ext. 5545

DISCLAIMER

This document was prepared as an account of work sponsored by the United States Government. While this document is believed to contain correct information, neither the United States Government nor any agency thereof, nor the Regents of the University of California, nor any of their employees, makes any warranty, express or implied, or assumes any legal responsibility for the accuracy, completeness, or usefulness of any information, apparatus, product, or process disclosed, or represents that its use would not infringe privately owned rights. Reference herein to any specific commercial product, process, or service by its trade name, trademark, manufacturer, or otherwise, does not necessarily constitute or imply its endorsement, recommendation, or favoring by the United States Government or any agency thereof, or the Regents of the University of California. The views and opinions of authors expressed herein do not necessarily state or reflect those of the United States Government or any agency thereof or the Regents of the University of California.

Presented by M. L. Stevenson at
the 1965 Boulder Conference on
Particle Physics, Boulder, Colorado,
Aug. 9-20, 1965 and
submitted to
Physical Reveiw

UCRL-16443

UNIVERSITY OF CALIFORNIA

Lawrence Radiation Laboratory
Berkeley, California

AEC Contract No. W-7405-eng-48

DECAY PROPERTIES OF THE ω MESON

Stanley M. Flatté, Darrell O. Huwe, Joseph J. Murray,
Janice Button-Shafer, Frank T. Solmitz, M. Lynn Stevenson,
and Charles Wohl

October 11, 1965

DECAY PROPERTIES OF THE ω MESON*

Stanley M. Flatté,† Darrel O. Huwe, Joseph J. Murray,
Janice Button-Shafer, Frank T. Solmitz, M. Lynn Stevenson,
and Charles Wohl

Lawrence Radiation Laboratory
University of California
Berkeley, California

October 11, 1965

ABSTRACT

The reaction $K^-p \rightarrow \Lambda\omega$, as observed in the Lawrence Radiation Laboratory's 72-inch hydrogen bubble chamber, has provided over 4600 examples of ω decay. The distribution of pion momenta in the decay $\omega \rightarrow \pi^+\pi^-\pi^0$, of which 4200 examples have been seen, is found to be consistent with C-conservation. With the assumption that the ω spin is 1^-, the pion-momentum distributions predicted by two different decay matrix elements are compared with the experimental distributions, as a test for final-state interactions. It is also shown that a spin of 3^- for the ω is unlikely. Branching fractions of other decay modes with respect to the $\pi^+\pi^-\pi^0$ decay mode are: neutrals, 0.097 ± 0.016; $\eta\gamma$, < 0.017; $\eta\pi^0$, < 0.017; $\pi^+\pi^-\gamma$, < 0.05; e^+e^-, < 0.0003; and $\mu^+\mu^-$, < 0.0017. The $\omega \rightarrow \pi^+\pi^-$ branching fraction lies between $(0.17 \pm 0.03)^2 = 0.029$ (coherence between the ρ and the ω production amplitudes assumed) and 0.082 ± 0.020 (incoherence assumed).

DECAY PROPERTIES OF THE ω MESON*

Stanley M. Flatté,† Darrell O. Huwe, Joseph J. Murray,
Janice Button-Shafer, Frank T. Solmitz, M. Lynn Stevenson,
and Charles Wohl

Lawrence Radiation Laboratory
University of California
Berkeley, California

October 11, 1965

I. INTRODUCTION

We present here some measurements of ω decay as seen in the reaction $K^-p \rightarrow \Lambda\omega$, with incident K^- momentum between 1.2 and 1.8 BeV/c. The decay modes studied provide information on C-conservation, SU(3) symmetry and ϕ-ω mixing, the electromagnetic structure of particles, I-conservation, and the spin of the ω.

The conservation of C forbids the decays $\omega \rightarrow \eta\pi^0$ and $\omega \rightarrow \rho\gamma$, and also forbids an asymmetry between the π^+ and π^- in the decay $\omega \rightarrow \pi^+\pi^-\pi^0$. Measurement of these properties therefore tests C-conservation. According to SU(3) symmetry, the ω is a vector meson that is a linear combination of ω_8, a member of an octet of vector mesons, and ω_1, an SU(3) singlet. The decay mode $\omega \rightarrow \eta\gamma$ bears upon this presumption, called ϕ-ω mixing.

The $\pi^+\pi^-$, $\pi^+\pi^-\gamma$, $\eta\gamma$, e^+e^-, and $\mu^+\mu^-$ decay modes of the ω have an intimate connection with the electromagnetic structure of mesons. The two-pi decay mode is crucial to an understanding of the possible electromagnetic mixing between ρ and ω.

The distribution over the internal-momentum variables in $\omega \rightarrow \pi^+\pi^-\pi^0$ allows us, because of our large amount of data, to look for final-state interactions and to explore the possibility that the ω spin is $J^P = 3^-$ rather than $J^P = 1^-$.

Table II summarizes the decay properties of the ω.

II. EXPERIMENTAL IDENTIFICATION OF THE REACTION

Approximately 4600 events of the reaction

$$K^- p \rightarrow \Lambda\omega$$

have been identified in a K^- exposure of the 72-inch hydrogen bubble chamber. The momentum settings were 1.22, 1.32, 1.42, 1.51, 1.60, and 1.70 BeV/c. The momentum spread at each momentum was 6%, full width at half maximum (FWHM). Threshold for $K^- p \rightarrow \Lambda\omega$ is 1.23 BeV/c. Table I summarizes the amount of data at each momentum setting in terms of the number of events per millibarn of cross section.

All events that we consider in this analysis have an identified $\Lambda \rightarrow p\pi^-$ decay that appears as a "V" in the chamber. The number of charged prongs that emerge from the production vertex depends on how the ω decays. The ω decay modes that are of interest to us are:

V + zero-prong (Fig. 1)

$\omega \rightarrow$ neutrals

V + two-prong (Fig. 2)

$\omega \rightarrow \pi^+\pi^-\pi^0$

$\pi^+\pi^-\gamma$

$\pi^+\pi^-$

η + (neutrals)

$\hookrightarrow \pi^+\pi^-\pi^0$

$\mu^+\mu^-$

e^+e^-

A. Λ + Neutrals

The V + zero-prong events in our experiment, including also momentum settings of 1.0 and 1.1 BeV/c, have been studied in detail by Wohl, Solmitz, and Stevenson.[1] We will touch upon the experimental methods concerning our use of the data.

Any V + zero-prong event whose V fits a three-constraint (3C) Λ decay with a chi-squared (χ^2) less than 30 is called a Λ event. If an event does not fit the (3C) hypothesis then a (1C) hypothesis is tried in which the Λ flight line is not constrained to pass through the production vertex. If the (1C) fit has a χ^2 less than 10 and the Λ flight line passes within 8 mm of the last bubble of the incident track, then the event is accepted as a Λ event. Approximately 3% of the good Λ events were accepted on the basis of the (1C) criteria. The length of the Λ path projected onto a horizontal plane in the bubble chamber is required to be greater than 3 mm. This requirement allows us to correct for the fact that some V + zero-prong events will be incorrectly called two prongs because the Λ path is too short. By ignoring Λ's with short path-lengths, we eliminate the uncertainty in the scanning bias and make it easy to correct for the number of true (Λ + neutral) events that we discard by this criterion.

We shall speak of the "Missing Mass" as the invariant mass of the system of undetected neutrals recoiling against the Λ. The identification of the reaction $K^-p \rightarrow \Lambda\,(\omega \rightarrow \text{neutrals})$ is achieved by plotting the (Missing Mass)^2 [$(MM)^2$] and observing the number of events that lie above the background in the region of $(0.784\ \text{BeV})^2 = 0.615\ \text{BeV}^2$. This number is discussed in Sec. III. A. Figure 3 displays the $(MM)^2$ distributions as a function of incident momentum from 1.0 to 1.7 BeV/c. The π^0, η, and ω neutral-decay modes can be seen at 0.02, 0.30, and 0.61 BeV^2, respectively.

B. Λ + two-Prongs

In this topology we find most of the ($\Lambda + \omega$) events. All V + two-prong events are fit to the hypotheses;

$$K^- + p \rightarrow \pi^+ + \pi^- + (\Lambda \rightarrow p + \pi^-) \quad (1)$$

$$K^- + p \rightarrow \pi^+ + \pi^- + (\Sigma^0 \rightarrow (\Lambda \rightarrow p + \pi^-) + \gamma) \quad (2)$$

$$K^- + p \rightarrow \pi^+ + \pi^- + \pi^0 + (\Lambda \rightarrow p + \pi^-) \quad (3)$$

$$K^- + p \rightarrow \pi^- + p + (\bar{K}^0 \rightarrow \pi^+ + \pi^-) \quad (4)$$

$$K^- + p \rightarrow \pi^- + p + \pi^0 + (\bar{K}^0 \rightarrow \pi^+ + \pi^-) \quad (5)$$

$$K^- + p \rightarrow \pi^- + \pi^+ + n + (\bar{K}^0 \rightarrow \pi^+ + \pi^-). \quad (6)$$

Other hypotheses, related to specific decay modes of the ω, are tried. These will be discussed in Sec. III.

The fitting of V + two-prongs to hypotheses (1) through (6) is done in two steps. First, the neutral V direction is taken to be the line connecting the primary vertex to the vertex of the V, and the V is fit to the two hypotheses, $\Lambda \rightarrow p + \pi^-$ and $K_1^0 \rightarrow \pi^+ + \pi^-$. These are three-constraint fits. If $\chi^2(\Lambda)$ is less than 20, reaction hypotheses (1), (2), and (3) are tried; and if $\chi^2(K_1^0)$ is less than 20, reaction hypotheses (4), (5) and (6) are tried. If $\chi^2(\Lambda)$ and $\chi^2(K^0)$ are each less than 20, all the production hypotheses (1) through (6) are tried; in this case, if a low chi-squared (less than 10 times the number of constraints) is obtained for some production process for <u>both</u> interpretations of the V, the event is classified as ambiguous between Λ and $\bar{K}^0$ production. The percentage of ambiguous events varied from 1.2% at 1.2 BeV/c to 2.5% at 1.7 BeV/c. We believe that most of these ambiguous events are Λ events because:

1. It is easier for a Λ decay to "fake" a K_1^0 decay than vice versa, because most K_1^0 decay fragments have a transverse momentum that exceeds the rest-frame momentum of the Λ decay fragments. More than 90% of the K_1^0's decay in just this way.

2. There are roughly twice as many Λ's as $\bar{K}^0$'s to begin with (see Table I).

Let us now consider the unambiguous Λ events. Events that simultaneously fit reactions (1) and (3) are less than 1% of the total number of Λ + two-prongs. Consequently the $\Lambda\pi^+\pi^-$ events can be cleanly separated from the $\Lambda\pi^+\pi^-\pi^0$ events. The task of separating reaction (2) from reaction (3) is not so simple. Although in both reactions a single neutral particle is missing, the γ ray and the Λ of (2) are constrained to have the Σ^0 mass while no similar constraint exists for the π^0 and Λ of reaction (3). Consequently reaction (2) is a two-constraint fit and reaction (3) is a one-constraint fit. Reaction (1) is a four-constraint fit. If our measurement errors were properly estimated and were free from systematic errors, the mean value of chi-squared would be equal to the number of the constraint class. Actually our errors are underestimated so that this equality does not hold in general.

The selection criteria for our $\Lambda\pi^+\pi^-\pi^0$ sample were

$$\chi^2(\Lambda 3\pi) \leq 10 \qquad \text{and,}$$

$$\chi^2(\Lambda 3\pi) \leq \frac{1}{2}\chi^2(\Sigma 2\pi) \qquad \text{and,}$$

$$\chi^2(\Lambda 3\pi) \leq \frac{1}{4}\chi^2(\Lambda 2\pi).$$

The reaction $K^- + p \rightarrow \Lambda + (\omega \rightarrow \pi^+\pi^-\pi^0)$ is identified by means of the peak at 780 MeV in the three-pion mass spectrum $M(\pi^+\pi^-\pi^0)$. Figure 4 displays this spectrum for all incident momenta.

III. DECAY PROPERTIES OF THE ω

A. $\pi^+\pi^-\pi^0$ Decay Mode

We discuss here those aspects of the ω decay that should be unrelated to the ω-production process, namely, the population of the Dalitz plot for the π^+, π^-, and π^0 decay fragments. Here x and y are defined in the usual way

$$x = \frac{T_- - T_+}{\sqrt{3}\,Q}$$

$$y = \frac{T_0}{Q}$$

where T_+, T_-, and T_0 are the kinetic energies of the pions in the three-pion rest frame and Q is the sum of the kinetic energies of all three pions.

Figure 5(a) displays the Dalitz plot for 5 658 events that fall in the 750- to 815-MeV peak region. Figure 5(b) is a similar plot for 2 978 events in both control regions, 685 to 750 MeV and 815 to 880 MeV.

1. Comparison of Data with Simplest Matrix Element

We compare the density of points on the Dalitz plot with predictions of the simplest matrix element for the T = 0, three-pion decay of a $J^{PG} = 1^{--}$ meson, namely,

$$|\mathcal{M}|^2 \propto |\underset{\sim}{p}_1 \times \underset{\sim}{p}_2 + \underset{\sim}{p}_2 \times \underset{\sim}{p}_3 + \underset{\sim}{p}_3 \times \underset{\sim}{p}_1|^2 \propto |\underset{\sim}{p}_1 \times \underset{\sim}{p}_2|^2 .$$

Here, $\underset{\sim}{p}_1$, $\underset{\sim}{p}_2$, and $\underset{\sim}{p}_3$ are the pion momenta in the ω rest system. The Dalitz plot is folded about the y axis (valid if C is conserved) and divided into nine sectors and ten radial zones as indicated in Fig. 5(c). The sectors each subtend an angle of twenty degrees. The zones are determined by the contour lines of equal intervals of $|\mathcal{M}|^2$ from 0.1 to 0.9 $|\mathcal{M}|^2_{max}$.

The numbers of events per subsector in the peak region and the control regions are determined. From Fig. 4 we estimate that there are 1 450 background events in the peak region. If we assume that the behavior of the

background events is similar to the average behavior of the events in the adjacent control regions then a background subtraction can be made on the peak-region events. However we have some misgivings that this assumption is, in general, a valid one. Nevertheless we make it. The number of events per subsector in the control regions is first multiplied by the ratio of total background events to total control-region events and then subtracted from the number of peak-region events per subsector. The resulting number of ω events in each subsector is then divided by the area of that subsector. The unit of area that we used is 900 times the unit of area in Dalitz variables (x, y). The results are summarized in Fig. 6(a), where the data are grouped according to zone number. Sectors of similar shape are given similar symbols in this plot, i.e., no symbols for sectors (1), (6), and (7), open circles for sectors (2), (5), and (8), and exes for sectors (3), (4), and (9).

As an afterthought, we questioned the method (described above) in which a single ratio of total background events to total control events was used to correct the different zones and sectors for background. Therefore, we made ten $M(\pi^+\pi^-\pi^0)$ histograms (similar to Fig. 4) corresponding to those events that fell in the ten radial zones illustrated in Fig. 5(c). From these curves we determined ten corresponding ratios of background to control events. Even though these ratios varied little from zone to zone, they were used in correcting for the background in the subsequent analysis.

From the work of Gelfand et al.[2] and Armenteros et al.,[3] the width of the ω is known to be 12 ± 2 MeV.[4] Thus the decay is neither electromagnetic nor weak, and hence isotopic spin is conserved in the decay. This conservation requires the matrix element to be totally antisymmetric with respect to the interchange of any pair of pions. Subsectors of similar shape should have

the same number of events. To within statistical uncertainty the data agree with this requirement.

Figure 6(b) displays the difference in number of events per unit area $N(x > 0) - N(x < 0)$ for each subsector of the Dalitz plot. This difference should be zero if C is conserved. Later we shall discuss possible violations of I and C in the data. For the moment we assume both I and C to be conserved.

We add sectors (1), (6), and (7) together; (2), (5), and (8) together; and (3), (4), and (9) together. The results are plotted in Fig. 7. The solid curves, labelled 1^-, are the theoretical curves of $|\mathcal{M}|^2$ normalized to the total number of ω's, vs the distance from the center of the Dalitz plot. The value of each curve at the center of the Dalitz plot is N_ω/V, where N_ω is the total number of ω events and V is the integral of $|\mathcal{M}|^2/|\mathcal{M}|^2_{max}$ over sectors (1), (2), and (3) of the Dalitz plot. The chi-squared fits to the theoretical curves are 4.9, 8.4, and 10.7 for sectors (1) + (6) + (7), (2) + (5) + (8), and (3) + (4) + (9), respectively. The combined chi-squared value is 24.0 (29 is expected). The probability of our getting a fit worse than this is 72.9%--this we refer to as the confidence level of the fit.

2. Test for Final-State Interactions

Even though the fit to the simplest matrix element is excellent, we have tried fitting the data to matrix elements of the form $|\mathcal{M}|^2 = F(M_{12}^2, M_{23}^2, M_{31}^2)\, |\underset{\sim}{p}_1 \times \underset{\sim}{p}_2|^2$, where M_{ij} is the effective mass of the two-pion system containing pions i and j.

$$F = \frac{1}{(M_{23}^2 - m_\rho^2) + i m_\rho \Gamma_\rho(M_{23})} + \text{cyclic},$$

where

$$\Gamma_\rho(M_{23}) = \frac{m_\rho}{M_{23}} \left\{ \frac{M_{23}^2 - 4m_\pi^2}{m_\rho^2 - 4m_\pi^2} \right\}^{3/2} \Gamma_{\rho 0}$$

$$\Gamma_{\rho 0} = \text{constant} = 100 \text{ MeV}$$

$$m_\rho = 750 \text{ MeV}.$$

Such a form was suggested by Gell-Mann[5] to account for the virtual decay $\omega \to \rho + \pi$. The largest value of $M(\pi^+\pi^-)$ is 642 MeV at $y = 0$, and 100 MeV away from the ρ pole at $y = -0.263$. The dashed curves of Fig. 7 [labelled $1^-(\rho\pi)$] give χ^2 values of 8.2, 5.4, 9.4 for sectors (1) + (6) + (7), (2) + (5) + (8), and (3) + (4) + (9), respectively. The total χ^2 is 22.9 when, as before, the expected value is 29.

The fit, as before, is excellent--it has a confidence level of 78.0%. Therefore, on the basis of these data it is not possible to distinguish between the two forms of the matrix element, 1^- or $1^-(\rho\pi)$.

3. <u>Can the Spin of the ω Be 3^- ?</u>

Zemach[6] has shown that the qualitative features of the three-pion Dalitz plot recur when the angular momentum is increased by two units. We have compared the data to $J^P = 3^-$ - matrix elements of the form

$$|\mathcal{M}|^2 = \sum_{ijk} |f_1(M_{23}^2)[T(11Q)]_{ijk} + \text{cyclic}|^2$$

where $T(11\,Q)$ is the traceless, symmetric third-rank tensor whose <u>ijk</u>th element is

$$[T(11\,Q)]_{ijk} = \frac{1}{3}\,[(p_1)_i\,(p_1)_j\,q_k + (p_1)_i\,q_j\,(p_1)_k + q_i\,(p_1)_j\,(p_1)_k]$$
$$- \frac{|\underset{\sim}{p}_1|^2}{15}\,(q_i\,\delta_{jk} + q_j\,\delta_{ik} + q_k\,\delta_{ij})$$

where i, j, and k run from 1 to 3 and

$$\underset{\sim}{q} = \underset{\sim}{p}_1 \times \underset{\sim}{p}_2.$$

The term $f_1(M_{23}^2)$ is a scalar function.

$$|\mathcal{M}|^2 = q^2 \Big\{ \frac{4}{5} (|f_1|^2 p_1^4 + |f_2|^2 p_2^4 + |f_3|^2 p_3^4)$$

$$+ 2 \operatorname{Re} f_1^* f_2 [(\underset{\sim}{p}_1 \cdot \underset{\sim}{p}_2)^2 - \frac{1}{5} p_1^2 p_2^2]$$

$$+ 2 \operatorname{Re} f_2^* f_3 [(\underset{\sim}{p}_2 \cdot \underset{\sim}{p}_3)^2 - \frac{1}{5} p_2^2 p_3^2]$$

$$+ 2 \operatorname{Re} f_3^* f_1 [(\underset{\sim}{p}_3 \cdot \underset{\sim}{p}_1)^2 - \frac{1}{5} p_3^2 p_1^2] \Big\} .$$

Two different forms of f have been used; in the first, f equals a constant; in the second, $f = 1/[M_{23}^2 - m_\rho^2 + i m_\rho \Gamma_\rho(M_{23})]$. The terms f_2 and f_3 are formed by cyclic permutation. The first form is the simplest form of the matrix element. The second form represents an attempt to account for a possible final-state interaction between two of the pions in a $(J^P = 1^-)$ final state.

The two predictions for the density of points on the Dalitz plot, shown in Fig. 7, are labelled 3^- and $3^-(\rho\pi)$, respectively. Neither form of the $(J^P = 3^-)$ matrix elements fits the data. Total chi-squared values are 207 and 99, respectively. Unlike the $J^P = 2^\pm$ matrix elements that give vanishing density at the center regardless of the form factors, the $(J^P = 3^-)$ matrix elements could accidentally have just the right form factors to give a good fit to the observed data. It is, therefore, difficult to justify a definitive statement that the spin is not 3^---it just seems unlikely. The broad width of 12 MeV for the ω would be independent evidence against $J^P = 3^-$.

4. Test of C-Conservation in $\omega \to \pi^+\pi^-\pi^0$ Decay

It has been suggested that the apparent CP violation of $K_2 \to \pi^+\pi^-$ decay, a $(|\Delta S| = 1)$ transition, might be explained by introduction into the Hamiltonian of an interaction which conserves parity and strangeness, but violates C.[7] For $|\Delta S| = 0$ transitions, as in ω and η decay, this interaction could

become large enough to be observed along with strong or electromagnetic interactions. Lee[8] proposed that the matrix element for ω decay might be of the form $\mathcal{M} = (\underset{\sim}{p}_1 \times \underset{\sim}{p}_2)(A + Be^{i\phi_B} r \sin\theta)$, where r is the distance from the center of the Dalitz plot and θ is the angle, measured clockwise from the point of maximum momentum for the π^0. The term ϕ_B is a measure of final-state interactions, and A and B are positive real numbers whose ratio B/A could be, according to Lee, as large as 10^{-2}. This is a very small effect to be observed even with 4200 ω decays. Nevertheless, we fitted our data to this form of matrix element. The fit, which was excellent, gave $B/A = 0.11 \pm 0.09$, and $\phi_B = 3 \pm 6$ radians (i. e., any ϕ_B gives a good fit.) The fit is completely consistent with $B = 0$. Figure 6(b) shows this fit compared to the data. The confidence level is 66% (chi-squared is 171, and 179 is expected). As we suspected, with our data we are unable to detect such a small effect as $B/A \approx 10^{-2}$.

B. Neutral-Decay Mode

Figure 3 shows the neutral decay of the ω. In Fig. 8, the 12 351 Λ zero-prong events at incident momenta 1.4, 1.5, 1.6, and 1.7 BeV/c have been combined to produce a $(\text{Missing-Mass})^2$ distribution. Only events with a projected length greater than 3 mm were plotted. The smooth curve drawn above the background curve in the ω region contains 359 events. Several independent estimates averaging 348 ± 55, were made on the basis of similar curves. The main uncertainty in this number, which has been included in the stated error, is in our estimate of the shape of the background curve. This number can be converted into a cross section for $K^-p \rightarrow (\omega \rightarrow \text{neutral}) + (\Lambda \rightarrow p\pi^-)$ averaged over the momentum distribution of the 1.4, 1.5, 1.6, and 1.7 BeV/c data; it is 0.061 ± 0.010 mb. The number contains corrections for:

(a) Scanning efficiency (3%),

(b) Number of Λ's that decay with a projected path length less than 3 mm (5.5%),

(c) Measurement failures that were not included in the sample (3%),

(d) Λ escape (1.5%),

(e) Dalitz decays at production vertex (1.25 %).

From a curve similar to Fig. 4 we obtain $K^-p \rightarrow (\omega \rightarrow \pi^+\pi^-\pi^0) + (\Lambda \rightarrow p\pi^-)$ events with a Λ path length greater than 2 mm at momenta of 1.4, 1.5, 1.6, and 1.7 BeV/c. The fiducial volume of the chamber was slightly different for the V + zero-prongs and the V + two-prongs. This number is converted to a cross section of 0.63 ± 0.04 mb (averaged over momenta from 1.4 to 1.7 BeV/c) for $K^- + p \rightarrow (\omega \rightarrow \pi^+\pi^-\pi^0) + (\Lambda \rightarrow p\pi^-)$.

The branching ratio of neutrals to $\pi^+\pi^-\pi^0$ is $\Gamma(\omega \rightarrow \text{neutral})/\Gamma(\omega \rightarrow \pi^+\pi^-\pi^0) = 0.097 \pm 0.016$.

C. $\omega \rightarrow \pi^+\pi^-$ Decay Mode

This mode of decay violates I-conservation. It has been discussed theoretically by many authors[9] and examined experimentally by others.[10]

The reactions

$$K^- + p \rightarrow (Y_1^{*\pm}(1382) \rightarrow \Lambda + \pi^\pm) + \pi \qquad (7)$$

dominate the topology of reaction (1) and make the identification of the reaction

$$K^- + p \rightarrow \Lambda + (\omega \rightarrow \pi^+ + \pi^-) \qquad (8)$$

difficult. Consequently we look only at type (1) events that could not be reaction (7). The unshaded region of Fig. 9 shows that portion of the $K^-p \rightarrow \Lambda\pi^+\pi^-$ Dalitz plot for 1.5 BeV/c in which we search for $\omega \rightarrow \pi^+\pi^-$. To increase our statistical accuracy, we combine all incident momenta together. At each momentum, as at 1.5 BeV/c, we require that the $\Lambda\pi^\pm$ mass be greater than 1490 MeV, a value which is four half-widths of the $Y^*(1382)$

from 1382 MeV. Figure 10(a) displays the $M^2(\pi^+\pi^-)$ histogram for 3887 events that satisfy the above criteria.

We first examine the possibility that the narrow peak near the ω mass might be a statistical fluctuation. The curve of Fig. 10(a) is the "least-square" solution to a single $\rho \to \pi^+\pi^-$ resonance superimposed upon a smooth background. The ρ amplitude has the form

$$A_\rho = \frac{m_\rho^{3/2}\,\Gamma_\rho^{1/2}}{(m_\rho^2 - M^2) - i m_\rho \Gamma_\rho}$$

$$\Gamma_\rho = \Gamma_{\rho 0}\,\frac{m_\rho}{M}\left(\frac{M^2 - 4m_\pi^2}{m_\rho^2 - 4m_\pi^2}\right)^{3/2},$$

where M is the invariant mass of the $\pi^+\pi^-$ system. The mass m_ρ and width $\Gamma_{\rho 0}$ of the ρ were allowed to vary along with three parameters representing the parabolic background. The fit, with $m_\rho = 762 \pm 4$ MeV and $\Gamma_{\rho 0} = 105 \pm 13$ MeV, is very poor. Chi-squared is 103.4 when 60 is expected. The confidence level (the probability of our getting a fit worse than this) is 0.04%. We reject the possibility that this is a statistical fluctuation. We have explored and ruled out the possibility that the $Y^*(1660)$ could have produced a peak in the ω region by its projection on the $M^2(\pi^+\pi^-)$ axis. Nor could coherent interference between ρ and background improve the fit appreciably.

The next possibility is that we are observing the decay $\omega \to \pi^+\pi^-$, a mode that many authors have commented on.[9,10] Here we are faced with the problem of ρ-ω interference in the quantum-mechanical sense; that is, the ρ and ω amplitudes lead to the same two-pion final state. The processes producing the final states may cause these amplitudes to add coherently, incoherently, or partly coherently. The mass distributions of any process in

which the amplitudes are partly coherent can be represented by a linear sum of a completely coherent distribution and a completely incoherent one. Therefore, because our statistics are limited, we consider only the two extreme possibilities--complete coherence and complete incoherence--realizing that the truth must lie somewhere between.

1. Complete Coherence

The curve in Fig. 10(b) shows the best-fit solution to the hypothesis of complete coherence. Chi-squared is 81.1 when 60 is expected. The confidence level is 3.7%. Two parameters, f and ϕ, are used to represent the relative magnitude and phase of the two superposed amplitudes for $\rho \to \pi^+\pi^-$ and $\omega \to \pi^+\pi^-$:

$$A = \left(A_\rho = \frac{m_\rho^{3/2}\Gamma_\rho^{1/2}}{(m_\rho^2 - M^2) - i m_\rho \Gamma_\rho}\right) + \left(A_\omega = \frac{f e^{i\phi} m_\omega^{3/2}\Gamma_\omega^{1/2}}{(m_\omega^2 - M^2) - i m_\omega \Gamma_\omega}\right) ,$$

$$\text{where } \Gamma_\rho = \Gamma_{\rho 0} \frac{m_\rho}{M} \left(\frac{M^2 - 4m_\pi^2}{m_\rho^2 - 4m_\pi^2}\right)^{3/2}$$

$$\Gamma_\omega = \Gamma_{\omega 0} \frac{m_\omega}{M} \left(\frac{M^2 - 4m_\pi^2}{m_\omega^2 - 4m_\pi^2}\right)^{3/2} .$$

Again three parameters are used to express the approximate form of the background (shown as a dashed line in Fig. 10b). Here, m_ρ, $\Gamma_{\rho 0}$, m_ω, and $\Gamma_{\omega 0}$ have been fixed at 750, 100, 782, and 9 MeV, respectively. Finally a resolution function of 10-MeV FWHM is folded into the theoretical curve.

To convert the value of f into a branching ratio, we must correct for the number of $(\omega \to \pi^+\pi^-)$ events that were excluded by not considering those events of topology similar to (7). The result of this correction yields

$$\Gamma(\omega \to \pi^+\pi^-)/\Gamma(\omega \to \pi^+\pi^-\pi^0) = (0.17 \pm 0.03)^2 = 2.9 \times 10^{-2}.$$

We quote the error in this strange way because we find that it is the amplitude f, not f^2, that is gaussianly distributed. Figure 11 shows a contour map of chi-squared plotted in terms of the real and imaginary parts of $fe^{i\phi}$. A second scale gives directly the amplitude $\Gamma^{1/2}(\omega \to \pi^+\pi^-)$ in units of $\text{MeV}^{1/2}$. The heavy ellipse-like contours marked for chi-squared values of 1, 4, and 9 correspond respectively to 1, 2, and 3 standard deviations from the best value of $\Gamma^{1/2}(\omega \to \pi^+\pi^-) = (0.25\ \text{MeV})^{1/2}$ and $\phi = 0.81$ radians. The dashed circle is the theoretical prediction by Coleman et al.[9] of $\Gamma^{1/2}(\omega \to \pi^+\pi^-) = (0.09\ \text{MeV})^{1/2}$ [or $\Gamma(\omega \to \pi^+\pi^-)/\Gamma(\omega \to \pi^+\pi^-\pi^0) = 1.1 \times 10^{-2}$]. The main contribution to this calculated rate comes from the diagrams that are possible if an octet of scalar mesons exists. This latter postulate is made in order to provide a specific mechanism for octet dominance in the eightfold way. If such terms are not included in their calculation a negligible rate of $\Gamma(\omega \to \pi^+\pi^-) = 0.0002$ MeV is predicted.

2. Complete Incoherence

The second of the two extreme possibilities is that ρ and ω are incoherent. This is perhaps closer to the truth because the data come from all incident momenta, from all momentum transfers, and from all decay angles. The best-fit solution, shown in Fig. 10(c), gives $\Gamma(\omega \to \pi^+\pi^-)/\Gamma(\omega \to \pi^+\pi^-\pi^0) = (8.2 \pm 2.0) \times 10^{-2}$. Chi-squared is 79.5 when 60 is expected; the confidence level is 4.7%. In this latter solution we allowed the ρ mass to vary rather than fixing it at 750 MeV. The best-fit value is $m_\rho = 740 \pm 7$ MeV. The mass of the ω has been fixed at 782 MeV with a width $\Gamma_{\omega 0} = 9$ MeV. The resolution function of 10-MeV width has been folded into all curves.

Finally, we note the compilation that Lütjens and Steinberger[11] made at a time when less than a quarter of our data was published.[12] They place an upper limit of $[\Gamma(\omega \to \pi^+\pi^-) = 0.07\ \text{MeV}]/\Gamma(\omega \to \pi^+\pi^-\pi^0) = 0.8 \times 10^{-2}$ with 90%

confidence. The number of $\omega \rightarrow \pi^+\pi^-\pi^0$ events that they compared with their $\pi^+\pi^-$ mass spectrum was 3541, of which 234 were from our data. (This number should properly have been 342.) The number of $\omega \rightarrow \pi^+\pi^-\pi^0$ in our experiment that should be compared with our $\pi\pi$ spectrum is 2330. [We have 4208 ($\omega \rightarrow \pi^+\pi^-\pi^0$) events. The correction for elimination of $Y^*(1385)$ from our $\pi^+\pi^-$ spectrum gives 4208/1.81 = 2330.] Perhaps it would be prudent to keep an open mind to other hypotheses that might explain our data. We feel that the enhancement in the ω region is not a statistical fluctuation. If it is a phenomenon that is unrelated to ω decay and if it does not interfere with the ρ meson, it would have its mass centered at about 789 MeV with a width of $\Gamma \approx 20$ MeV. The production-angle distribution in the ρ region does not differ significantly from that in the ω region. We can examine the production-angle distribution of the events in the enhancement by assuming that the background behaves like the adjoining regions and subtracting the distributions in the appropriate proportions. We find that the production-angle distribution so obtained resembles the $K^-p \rightarrow \Lambda + (\omega \rightarrow \pi^+\pi^-\pi^0)$ production-angle distribution. (See Fig. 12.)

D. Search for $\omega \rightarrow (\eta \rightarrow \pi^+ + \pi^- + \pi^0)$ + Neutrals

Events of this type are kinematically underdetermined, but in general fail to fit the overdetermined reactions

$$K^-p \rightarrow \Lambda\,\pi^+\pi^- \qquad (1)$$

$$K^-p \rightarrow \Sigma^0\pi^+\pi^- \qquad (2)$$

$$K^-p \rightarrow \Lambda\,\pi^+\pi^-\pi^0. \qquad (3)$$

Figure 13(a) is a histogram of the invariant-mass-squared of the system that recoils against the Λ for those events that fail to fit reactions (1), (2), and (3). The events are further required to have a missing mass greater than a π^0 mass. Fewer than 30 events occur above the background in the ω-mass

region of Fig. 13(a), as indicated by the arrow. Figure 14(b) is a similar plot for events with $\delta(\mathrm{mm})^2 < 6000\ \mathrm{MeV}^2$ (that is, well-measured events). Some events of the type $K^- + p \rightarrow \Lambda + (\omega \rightarrow \pi^+\pi^-\pi^0)$ are expected to have pions that scatter or decay in flight in an unobservable fashion and consequently fail to fit reaction (3). We estimate that 10 events of this type are in the ω region of Fig. 13(a). Hence, in our data there are fewer than 20 events of the type $\omega \rightarrow \pi^+ + \pi^- + x^0$, where x^0 is a neutral system with effective mass greater than the mass of the π^0. The decay $\omega \rightarrow (\eta \rightarrow \pi^+ + \pi^- + \pi^0)$ + neutrals is included in this type. Using the known branching ratio[13] $\Gamma(\eta \rightarrow \pi^+ + \pi^- + \pi^0)/\Gamma(\eta \rightarrow \text{all modes}) = 0.274$, we determine that there are fewer than 73 events of the type $\omega \rightarrow (\eta \rightarrow \text{all modes})$ + neutrals. Consequently, $\Gamma[\omega \rightarrow \eta\ (\text{all modes}) + \text{neut}]/\Gamma(\omega \rightarrow \pi^+ + \pi^- + \pi^0) < [(73/4\ 208) = 1.7 \times 10^{-2}]$. This number is important because it forms the upper limit of (a) the C-invariance violating decay mode $\omega \rightarrow \eta + \pi^0$, and (b) the electromagnetic decay mode $\omega \rightarrow \eta + \gamma$.

The branching ratio[4] $\Gamma(\eta \rightarrow \text{neut})/\Gamma(\eta \rightarrow \text{all modes}) = 0.67$ allows us to set an upper limit on one of the contributions to the neutral-decay mode of the ω: $\Gamma[\omega \rightarrow (\eta \rightarrow \text{neut}) + \text{neut}]/\Gamma(\omega \rightarrow \pi^+ + \pi^- + \pi^0) < 1.1 \times 10^{-2}$.

Glashow and Sommerfield[14] show that if the C-invariance-violating $\omega\eta\pi$ coupling-constant were the same as the $\rho\pi\pi$ coupling constant, then $\Gamma(\omega \rightarrow \eta + \pi^0) = 9.3$ MeV. Our experiment places an upper limit of $(0.017)(8.5\ \mathrm{MeV}) = 0.14$ MeV. Hence the C-nonconserving $\omega\eta\pi$ coupling can be compared to the C-conserving $\rho\pi\pi$ coupling: $G^2(\omega\eta\pi(/G^2(\rho\pi\pi) < 1.5 \times 10^{-2}$.

In his Varenna lectures (1964), Glashow[15] points out that measurements of $\omega \rightarrow \eta\gamma$, $\phi \rightarrow \pi^0\gamma$, and $\phi \rightarrow \eta\gamma$ can provide tests of the $\phi - \omega$ mixing theory. His predictions are $\Gamma(\omega \rightarrow \eta\gamma) \approx 0.002\ (1-5\epsilon)^2$ MeV, $\Gamma(\phi \rightarrow \pi^0 + \gamma) \approx 2.1\epsilon^2$ MeV, and $\Gamma(\phi \rightarrow \eta + \gamma) \approx 0.26(1 + 0.2\epsilon)^2$ MeV, where

ϵ is the ratio of the $\phi\rho\pi$ coupling constant $G(\phi\rho\pi)$ to the $\omega\rho\pi$ coupling constant $G(\omega\rho\pi)$. The quantity $|\epsilon| \equiv |G(\phi\rho\pi)/G(\omega\rho\pi)|$ is known to be less than 0.2 from the observed rates $\Gamma(\phi \to 3\pi) \leq (1/15)\Gamma(\omega \to 3\pi)$. Thus $\Gamma(\omega \to \eta + \gamma)$ could be zero if $\epsilon = +0.2$, and could be 0.008 MeV if $\epsilon = -0.2$. Both are consistent with our result of < 0.14 MeV.

E. Search for $\omega \to \pi^+ + \pi^- + \gamma$

This mode of decay is harder to identify because events of types (1), (2), and (3) with large measurement errors can simulate it. Therefore we select "good events," that is, those whose error in the square of the missing mass $[\delta(\mathrm{mm})^2]$ is less than 6000 MeV^2. Histograms of those events that are (a) poor fits to (1), (presumably those events are of the type $K^- + p \to \Lambda + \pi^+ + \pi^- + x^0$) and (b) have an invariant mass $M(\Lambda x^0) > 1250$ MeV (a value sufficient to exclude most Σ^0 events) are plotted in Fig. 14(a), (b), and (c). Only events with $M(\pi^+\pi^- x^0)$ in the ω-mass region (750 to 810 MeV) are shown in Fig. 14(c). Figures 14(a) and 14(b) are corresponding histograms for events in the η region (510 to 580 MeV) and for events between the η and ω regions (580 to 750 MeV). We find evidence for $\eta \to \pi^+ + \pi^- + (x^0 = \gamma)$ and for $\eta \to \pi^+ + \pi^- + (x^0 = \pi^0)$ in Fig. 14(a). We see evidence also of Σ^0 events [see Fig. 14(b)] not excluded by our criteria. In Fig. 14(c) we find no evidence for $\omega \to \pi^+ + \pi^- + (x^0 = \gamma)$. Fewer than 24 $\omega \to \pi^+\pi^-(x^0 = \gamma)$ events are in the vicinity of zero $(\mathrm{mm})^2$. From this number we determine that $\Gamma(\omega \to \pi^+\pi^-\gamma)/\Gamma(\omega \to \pi^+\pi^-\pi^0) < 0.05$. This result supersedes the value 0.032 ± 0.013 reported previously (Shafer et al.[16]) on a partial sample of the present data. At $(\mathrm{mm})^2 = 0$ they observed a small narrow peak, which they interpreted as $\omega \to \pi^+ + \pi^- + \gamma$. Subsequently, the addition of more data showed a larger and anomalously narrow peak; it vanished when the events in the peak were remeasured.

How this peak, much narrower than the resolution function (that vanishes upon remeasurement), came about remains a mystery. Singer's predictions[17] of this ratio are much smaller than the present limit.

F. Search for $\omega \to e^+e^-$ and $\omega \to \mu^+\mu^-$

Several authors[18] have pointed out the usefulness of a measurement of the $\omega \to e^+e^-$ and $\omega \to \mu^+\mu^-$ decay rates. The experimental measurements to date (see Table II) are consistent with (a) the "equivalence" of the electron and the muon; (b) no breakdown of quantum electrodynamics; and (c) the currently accepted role of the ω in the isoscalar nucleon form factor.

In our "standard" data-analysis system for V + two-prongs, the hypotheses $K^-p \to \Lambda + (\omega \to e^+e^-, \mu^+\mu^-)$ are not included. (See Sec. II.) We must therefore determine what happens to events of the type $K^-p \to \Lambda + (\omega \to e^+e^+, \mu^+\mu^-)$ in our data-analysis system. The program FAKE,[19] which generates events of any desired topology, generated events of the type $K^-p \to \Lambda + (\omega \to e^+e^-)$ with a production-angle distribution the same as that of the $K^-p \to \Lambda + (\omega \to \pi^+\pi^-\pi^0)$ events in our experiment. These FAKE-generated events were fitted to the same hypotheses as those to which our experimental events were fitted, and 412 out of 484 failed to fit all hypotheses. Therefore, we could expect (412/484) of the true $K^-p \to \Lambda + (\omega \to e^+e^-)$ events in our experiment to be in the sample that we call "failing" events. In our entire sample of V + two-prongs there were approximately 2000 "failing" events. These were fitted to the hypothesis $K^-p \to \Lambda\, e^+e^-$, and the effective mass of the e^+e^- system was plotted for those events with $\chi^2 < 20$. The resulting histogram is shown in Fig. 15(a). Exactly the same procedure was used for the $K^-p \to \Lambda + (\omega \to \mu^+\mu^-)$ events, where only 79 out of 489 events were expected to be in the "failing" category. The result of fitting the hypothesis $K^-p \to \Lambda\mu^+\mu^-$ to the failing events is shown in Fig. 15(b).

The mass spectra of Fig. 15(a) and (b) show no enhancements at the ω mass and we can therefore set an upper limit on the $\omega \rightarrow e^+e^-$ and $\omega \rightarrow \mu^+\mu^-$ decay rates. Our mass resolution is about 15 MeV (FWHM), which is much narrower than the bin sizes in Fig. 15. We can in fact set an upper limit of one ω event in each of the distributions of Fig. 15. In our experiment there are 4200 events of the type $K^-p \rightarrow (\Lambda \rightarrow p\pi^-) + (\omega \rightarrow \pi^+\pi^-\pi^0)$; therefore we find $\Gamma(\omega \rightarrow e^+e^-)/\Gamma(\omega \rightarrow \pi^+\pi^-\pi^0) < (1/4200)(484/412) < 0.0003$ and $\Gamma(\omega \rightarrow \mu^+\mu^-)/\Gamma(\omega \rightarrow \pi^+\pi^-\pi^0) < (1/4200)(489/79) < 0.0017$. The latest measurements, by Zdanis et al.,[20] are $\Gamma(\omega \rightarrow e^+e^-)/\Gamma(\omega \rightarrow \pi^+\pi^-\pi^0) \approx 0.0001$ and $\Gamma(\omega \rightarrow \mu^+\mu^-)/\Gamma(\omega \rightarrow \pi^+\pi^-\pi^0) < 0.001$.

We have ignored the possibility that we could see the remaining 15% of the $K^-p \rightarrow \Lambda + (\omega \rightarrow e^+e^-)$ events and the remaining 84% of the $K^-p \rightarrow \Lambda + (\omega \rightarrow \mu^+\mu^-)$ events in the sample that passes some "standard" hypothesis. We found that consideration of these events was impractical because of the large background.

IV. SUMMARY

We have tested C-conservation in three ways. First, we have shown $\Gamma(\omega \to \eta\pi^0)/\Gamma(\omega \to \pi^+\pi^-\pi^0) < 0.017$. Since $\omega \to \eta\pi^0$ would violate I-conservation if it took place, we would expect its rate to be of the order of α^2 times the $\omega \to \pi^+\pi^-\pi^0$ rate. Second, we have shown $\Gamma(\omega \to \rho\gamma)/\Gamma(\omega \to \pi^+\pi^-\pi^0) < 0.05$. We expect this fraction to be of order α even if C is violated. Third, we have tested the $\omega \to \pi^+\pi^-\pi^0$ Dalitz plot for an asymmetry between the π^+ and π^-, and have found it to be zero within the statistical error, which is about a few percent. Since such an asymmetry would violate I-conservation, we expect it to be of order α. Thus our tests of C are not very sensitive to electromagnetic violations, and we see that testing current theories on C in ω decay requires a great deal more data.

We have shown that it would take a very fortuitous combination of form factors for the spin of the ω to be 3^-, and that we do not have enough data to test for final-state interactions among the pions, specifically the ρ coupling.

In determining the $\omega \to \pi^+\pi^-$ rate, we were faced with the problem of ρ-ω interference. We treated the data in two extreme ways: First we assumed complete coherence in the production of ρ and ω, and second we assumed complete incoherence. The first way gave $\Gamma(\omega \to \pi^+\pi^-)/\Gamma(\omega \to \pi^+\pi^-\pi^0) = 0.029$; the second gave 0.082. The events in the peak at the ω mass in the two-pion mass spectrum have a production-angle distribution consistent with that of the ω.

Table II presents the decay rates we have measured.

ACKNOWLEDGMENTS

We thank Professor Luis W. Alvarez, Professor Samuel M. Berman (Stanford Linear Accelerator), Professor T. D. Lee (Columbia University), Professor Sheldon L. Glashow, Professor Robert H. Socolow, and Professor Charles Zemach for their motivation and interesting discussions. We also thank the members of the Scanning and Measuring group for their important contributions to the work.

FOOTNOTES AND REFERENCES

*Work done under the auspices of the U. S. Atomic Energy Commission.

†National Science Foundation Predoctoral Fellow.

1. C. G. Wohl, F. T. Solmitz, and M. L. Stevenson, The Reactions $K^- + p \rightarrow \bar{K}^0 + n$ and $K^- + p \rightarrow \Lambda + \pi^0$ from 1.2 to 1.7 GeV/c and Evidence for the Formation of a T = 1 Hyperon Resonance with Mass 2050 MeV and Spin-Parity $7/2^+$, Lawrence Radiation Laboratory Report UCRL-16484 (1965) (to be submitted to The Physical Review).

2. N. Gelfand, D. Miller, M. Nussbaum, J. Ratan, J. Schultz, J. Steinberger, T. -H. Tan, L. Kirsch, and R. Plano, Phys. Rev. Letters 11, 436 (1963). See also, D. C. Miller, Nevis Laboratory Report No. 131, 1965 (unpublished).

3. R. Armenteros, D. Edwards, T. Jacobsen, A. Shapira, J. Vandermeulen, Ch. D'Andlau, A. Astier, P. Baillon, H. Briand, J. Cohen-Ganouna, C. Defoix, J. Siand, C. Ghesquire, and P. Rivet, Proceedings of the Sienna International Conference on Elementary Particles, (Societa Italiana di Fisica, Bologna, Italy, 1963), p. 296; see reference 4.

4. Data on Elementary Particles and Resonant States, as compiled by A. Rosenfeld, A. Barbaro-Galtieri, W. Barkas, P. Bastien, J. Kirz, and M. Roos, (to be published in Oct. 1965 Rev. Mod. Phys.).

5. M. Gell-Mann, (California Institute of Technology) private communication, 1961.

6. C. Zemach, Phys. Rev. 133, B1201 (1964).

7. T. D. Lee and L. Wolfenstein, Phys. Rev. 138, B1490 (1965); J. Prentki and M. Veltman, Phys. Letters 15, 88 (1965); L. Okun, "Remark on CP-Parity", Institute of Theoretical and Experimental Physics Report Number 360, Moscow, 1964.

8. T. D. Lee, Phys. Rev. 139, B1415 (1965).

9. S. Fubini, Phys. Rev. Letters 7, 466 (1961); S. Glashow, Phys. Rev. Letters 7, 469 (1961); R. Jacob and R. G. Sachs, Phys. Rev. 121, 350 (1961); Y. Nambu and J. Sakurai, Phys. Rev. Letters 8, 79 (1962); G. Feinberg, Phys. Rev. Letters 8, 151 (1962); M. Gell-Mann, D. Sharp, and W. Wagner, Phys. Rev. Letters 8, 261 (1962); J. Bernstein and G. Feinberg, Nuovo Cimento 25, 1343 (1962), J. Harte and R. G. Sachs, Phys. Rev. 135, B459 (1964); S. Coleman, S. L. Glashow, H. J. Schnitzer, and R. Socolow, Proceedings of the International Conference on High Energy Physics, Dubna, 1964 (to be published); L. E. Picasso, L. A. Radicati, D. P. Zanello, and J. J. Sakurai, Nuovo Cimento 37, 187 (1965).

10. Janice Button, George R. Kalbfleisch, Gerald R. Lynch, Bogdan C. Maglić, Arthur H. Rosenfeld, and M. Lynn Stevenson, Pion-Pion Interaction in the Reaction $\bar{p} + p \rightarrow 2\pi^+ + 2\pi^- + n\pi^0$, Lawrence Radiation Laboratory Report UCRL-9814, 1961 (unpublished); C. Alff, D. Berley, D. Colley, N. Gelfand, U. Nauenberg, D. Miller, J. Schultz, J. Steinberger, T.-H Tan., H. Brugger, P. Kramer, and R. Plano, Phys. Rev. Letters 9, 322 (1962); W. J. Fickinger, D. K. Robinson, and E. O. Salant, Phys. Rev. Letters 10, 457 (1963); Saclay-Orsay-Bari-Bologna Collaboration Nuovo Cimento 29, 515 (1963); B. Buschbeck-Czapp, I. Wacek, W. A. Cooper, A. Friedman, E. Malamud, G. Otter, E. Gelsema, and A. Tenner, Proceedings of the Sienna Conference on Elementary Particles, Sienna, Italy 1963; J. J. Murray, Jr., M. Ferro-Luzzi, D. Huwe, J. Shafer, F. Solmitz, and M. Lynn Stevenson, Phys. Letters 7, 358 (1963); R. Armenteros et al., see reference 3; W. D. Walker, J. Boyd, A. R. Erwin, P. H. Satterblom,

M. A. Thompson, and E. West, Phys. Letters 8, 208 (1964); G. Lütjens and J. Steinberger, Phys. Rev. Letters 12, 51 (1964); D. O. Huwe, Study of the Reaction $K^- + p \rightarrow \Lambda + \pi^+ + \pi^-$ from 1.2 to 1.7 BeV/c, Lawrence Radiation Laboratory Report UCRL-11291 (1964); R. Kraemer, L. Madansky, M. Meer, M. Nussbaum, A. Pevsner, C. Richardson, R. Strand, R. Zdanis, T. Fields, S. Orenstein, and T. Toohig, Phys. Rev. 136, B496 (1964); J. P. Baton, A. Berthelot, B. Deler, O. Goussu, M. Neveu-Rene, A. Rogozinski, F. Shively, V. Alles-Borelli, E. Benedetti, R. Gessaroli, and P. Waloschek, Nuovo Cimento 35, 713 (1965); and S. Flatté, D. Huwe, J. Murray, J. Button-Shafer, F. Solmitz, M. Stevenson, and C. Wohl, Phys. Rev. Letters 14, 1095 (1965).

11. G. Lütjens and J. Steinberger, see reference 10.

12. J. J. Murray, Jr., et al. See reference 10.

13. E. C. Fowler, F. S. Crawford, Jr., L. J. Lloyd, R. A. Grossman, and L. Price, Phys. Rev. Letters 10, 110 (1963); H. Foelsche and H. Kraybill, Phys. Rev. 134, B1138 (1964); see reference 4.

14. S. L. Glashow and C. Sommerfield, Phys. Rev. Letters 15, 78 (1965).

15. S. L. Glashow, Proceedings of the International School of Physics, "Enrico Fermi", Varenna, Italy, 1964 (Academic Press, Inc., New York, to be published).

16. J. B. Shafer, J. J. Murray, M. Ferro-Luzzi, and D. O. Huwe, Proceedings of the International Conference on Nucleon Structures, Stanford University, 1963, Ed., R. Hofstadter and L. I. Schiff (Stanford University Press, Stanford, California, 1964), p. 386.

17. P. Singer, Phys. Rev. 128, 2789 (1962).

18. G. Feldman, T. Fulton, and K. C. Wali, Nuovo Cimento 24, 278 (1962); Y. Nambu and J. J. Sakurai, Phys. Rev. Letters 8, 79 (1962); M. Gell-Mann, D. Sharp, and W. Wagner, Phys. Rev. Letters 8,261 (1962); E. D. Zhizhin and V. V. Solov'ev, Proceedings of the International Conference on High-Energy Physics,(CERN, Geneva, 1962) p. 493; R. F. Dashen, and D. H. Sharp, Phys. Rev. 133, B1585 (1964).

19. G. R. Lynch, "Program FAKE: Monte Carlo Simulation of Bubble Chamber Events," Lawrence Radiation Laboratory Report UCRL-10335, 1962 (unpublished).

20. R. A. Zdanis, L. Mandansky, R. W. Kraemer, S. Hertzbach, and R. Strand, Phys. Rev. Letters 14,721 (1965).

Table I. Path lengths of K^- particles in our experiment.

	P_{K^-} (BeV/c)					
	1.22	1.32	1.42	1.51	1.60	1.69
Path length (events/mb)	1230 ± 60	1440 ± 70	825 ± 40	5085 ± 200	715 ± 35	1100 ± 55
V + two-prong events	4013	5411	3419	22,641	2,926	5,211
Λ two-prong events	2,922	3,798	2,225	15,007	1,674	3,225
V + zero-prong events[a]	3,721	-	2,854	18,659	2,463	3,683
Λ zero-prong events[a]	1,808	-	1,332	8,382	1,064	1,587

a The fiducial volume for V + zero-prongs was slightly different from that for V+two-prongs.

Table II. Decay modes of the ω meson

Decay mode of ω	Rate[a]	
	Other experiments[4]	This experiment
$\pi^+\pi^-\pi^0$	12 MeV	-
All neutrals	0.106 ± 0.010	0.097 ± 0.016
$\pi^0\gamma$	≈ 0.10	-
$\eta\gamma \rightarrow$ neutrals	-	< 0.011
$\pi^+\pi^-$, complete incoherence assumed	< 0.008[11]	0.082 ± 0.02
complete coherence assumed		$(0.17 \pm 0.03)^2 = 0.029$
$\pi^+\pi^-\gamma$	-	<0.05
$\eta\gamma$	-	< 0.017
$\eta\pi^0$	-	< 0.017
e^+e^-	≈ 0.0001	< 0.0003
$\mu^+\mu^-$	< 0.001	< 0.0017

[a] All fractions represent the absolute rate divided by the $\omega \rightarrow \pi^+\pi^-\pi^0$ rate.

FIGURE CAPTIONS

Fig. 1. V + zero-prong event.

Fig. 2. V + two-prong event.

Fig. 3. (Missing Mass)^2 distributions from the reaction $K^-p \rightarrow \Lambda$ + (Missing Mass) in the form of invisible neutrals. The distributions do not have a common normalization. The figure conveys only the shapes of the distributions.

Fig. 4. Three-pion mass spectrum from $K^-p \rightarrow \Lambda\pi^+\pi^-\pi^0$ with K^- momentum between 1.2 and 1.8 BeV; 10,242 events.

Fig. 5. Dalitz plot of the $\pi^+\pi^-\pi^0$ system in $K^-p \rightarrow \Lambda\pi^+\pi^-\pi^0$ showing the divisions into sectors and zones as explained in the text.

(a) Events with the mass of the three-pion system between 750 and 815 MeV. (b) Events with the three-pion mass between 685 and 750 or 815 and 880 MeV. (c) Division of the Dalitz plot into zones (separated by contours of $|\vec{p}_1 \times \vec{p}_2|^2$) and sectors (separated by equally spaced radial lines). (d) Folding of the Dalitz plot by sectors.

Fig. 6. (a) Density of points on $\omega \rightarrow \pi^+\pi^-\pi^0$ Dalitz plot.

(b) Test of C - conservation in ω decay: For each zone the difference, in number of events per unit area, between each of the nine sectors on one side of the Dalitz plot ($x > 0$) and their counterpart on the other side ($x < 0$) has been plotted. Sec. III. A explains the curves.

Fig. 7. Spin and parity of the ω. Density of events as a function of the distance from the center of the ω Dalitz plot.

Fig. 8. Distribution of (Missing Mass)^2 from $K^-p \rightarrow \Lambda$ + neutrals. K^- momenta from 1.4 to 1.7 BeV; 12,351 events.

Fig. 9. Dalitz plot of the $\Lambda\pi^+\pi^-$ system in $K^-p \rightarrow \Lambda\pi^+\pi^-$ for K^- momentum of 1.5 BeV/c. The unshaded region contains the events used in the search for the $\omega \rightarrow \pi^+\pi^-$ decay.

Fig. 10. Histogram of $M^2(\pi^+\pi^-)$ for $K^-p \rightarrow \Lambda\pi^+\pi^-$ events that are not $K^-p \rightarrow Y_1^*(1385) + \pi$; 1.0 to 1.8 BeV/c; 3887 events.

(a) The solid curve is the fit to ρ alone; the phase-space (dashed) curve is normalized to the total number of background events. The other dashed curve is the background curve (assumed to be parabolic).

(b) The solid curve is the fit to ρ and ω with completely coherent amplitudes; the dashed curve is background.

(c) The solid curve is the fit to ρ and ω with completely incoherent amplitudes; the dashed curve is background.

Fig. 11. Chi-squared contours for $\omega \rightarrow \pi^+\pi^-$ amplitude in $K^-p \rightarrow \Lambda\omega$; K^- momenta from 1.2 - 1.8 BeV/c.

Fig. 12. Comparison of the production-angle distributions of the ω decaying into $\pi^+\pi^-\pi^0$ and the ω decaying into $\pi^+\pi^-$. The distributions have been normalized to the same total area and background has been subtracted in both cases.

Fig. 13. (a) Histogram of the invariant mass of the system that recoils against the Λ for 1461 events that fail to fit the final states $\Lambda\pi^+\pi^-$, $\Lambda\pi^+\pi^-\pi^0$, and $\Sigma^0\pi^+\pi^-$.

(b) Only those 412 events are plotted whose error in (missing mass)^2 is less than 6000 MeV^2.

Fig. 14. Histogram of the (missing mass)^2 for "good events" [$\delta(\text{mm})^2 < 6000\ \text{MeV}^2$] that fail $\Lambda\pi^+\pi^-$ and $\Sigma^0\pi^+\pi^-$.

(a) Events with an invariant mass ($\pi^+\pi^-$ + neutrals) in the η region, 510 to 580 MeV;

(b) Events between the η and ω regions, namely, 580 to 750 MeV;

(c) Events in the ω mass region, 750 to 810 MeV.

Fig. 15. (a) Distribution of the e^+e^- invariant mass for the 14 events that fail the non-leptonic hypothesis and have $\chi^2(K^-p \to \Lambda e^+e^-) < 20$. The events near zero mass probably come from events of the type $K^-p \to \Lambda + (\pi^0 \to e^+e^-\gamma)$ that fit $K^-p \to \Lambda e^+e^-$.

(b) Distribution of the $\mu^+\mu^-$ invariant mass for the 25 events that fail the non-leptonic hypothesis and have $\chi^2(K^-p \to \Lambda\mu^+\mu^-) < 20$.

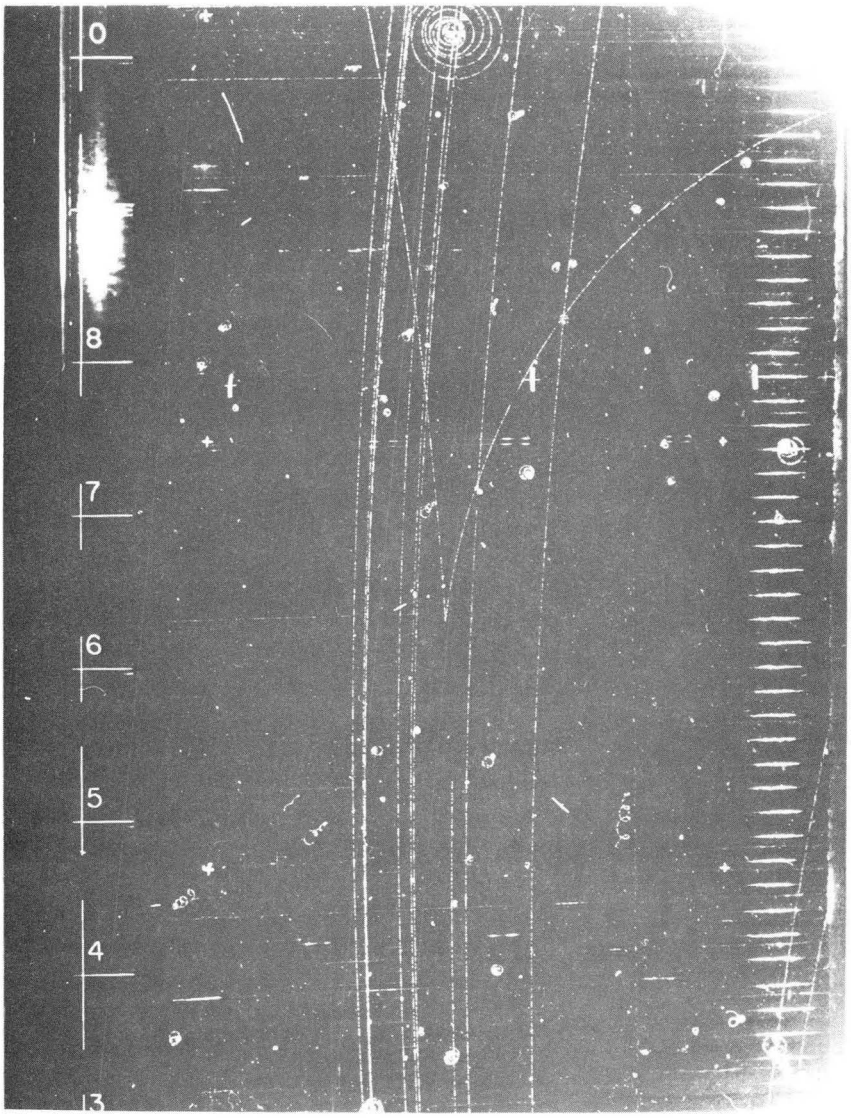

ZN-5251

Fig. 1

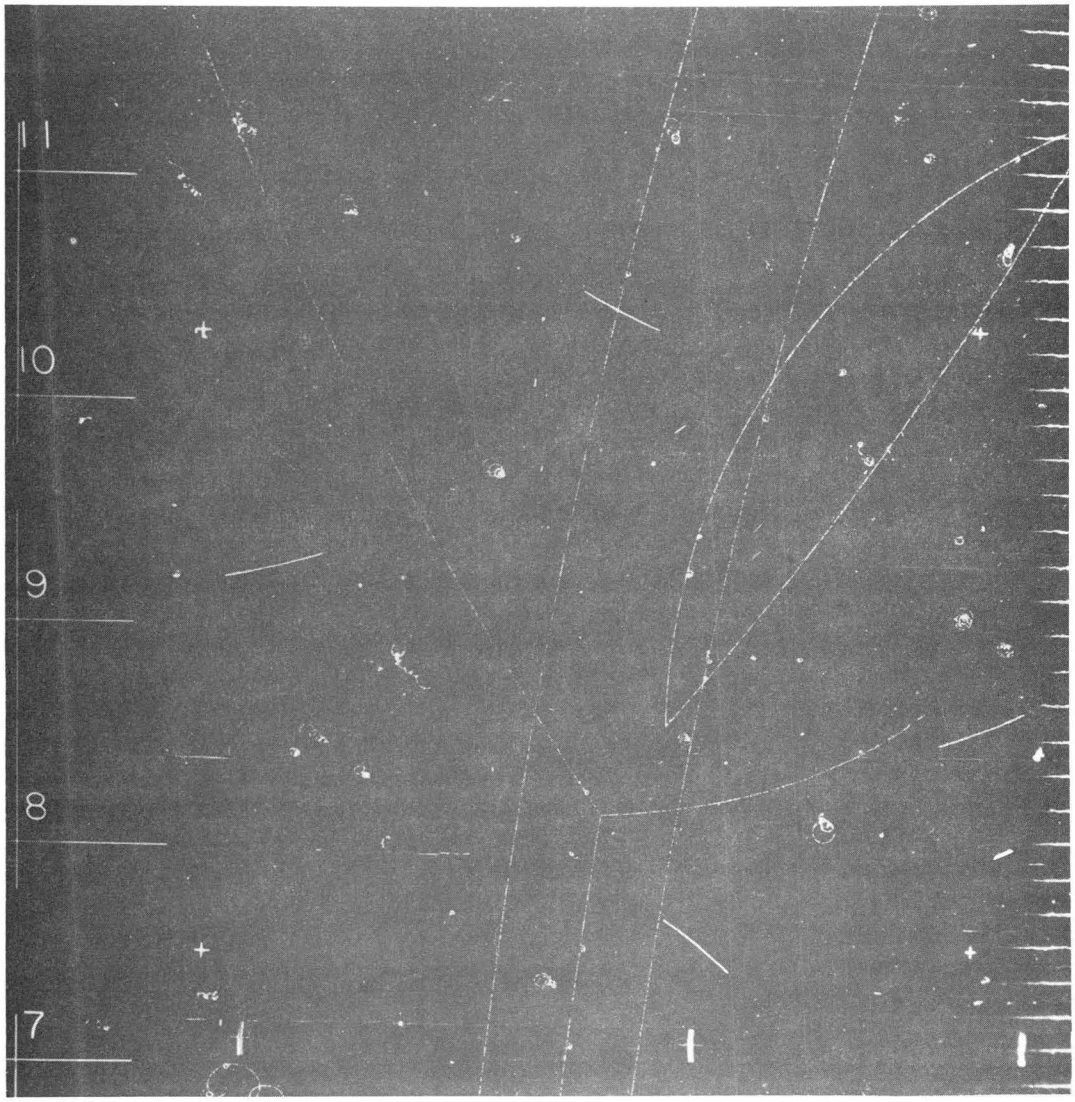

ZN-5235

Fig. 2

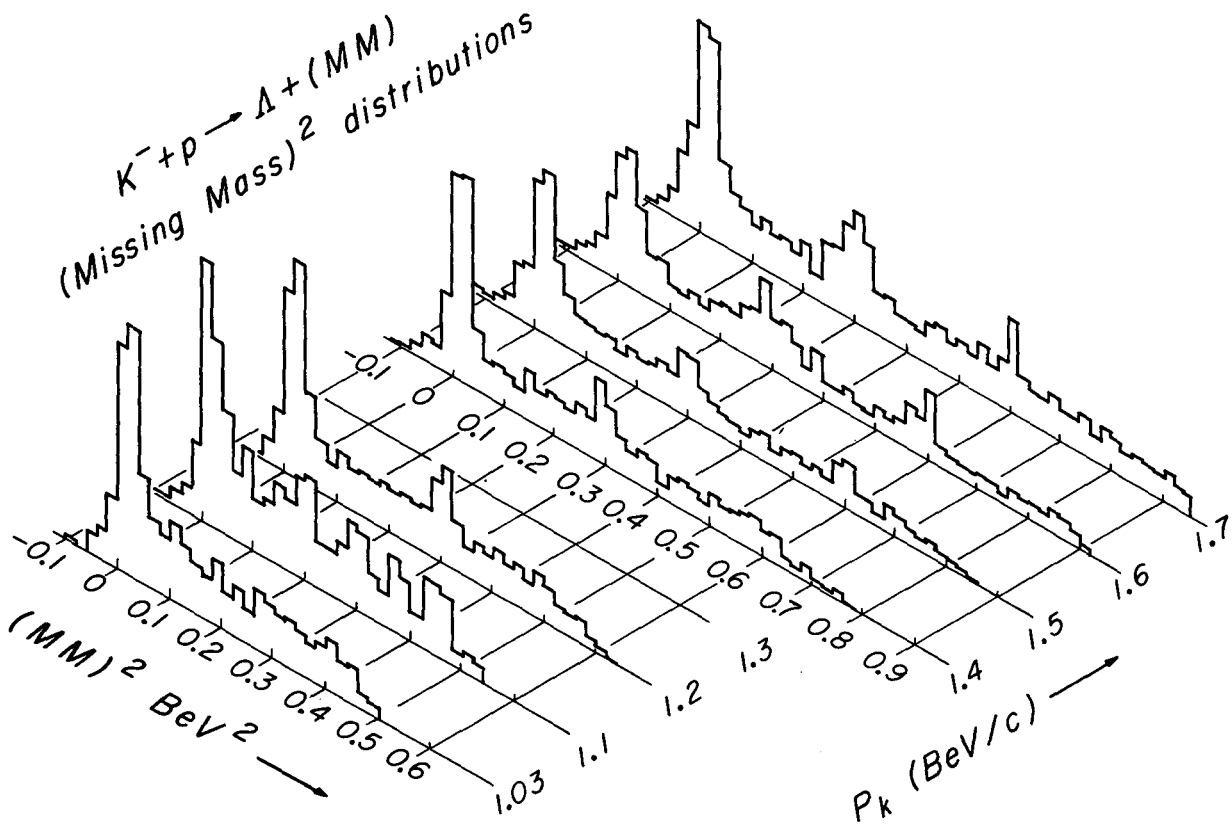

MUB-2581

Fig. 3

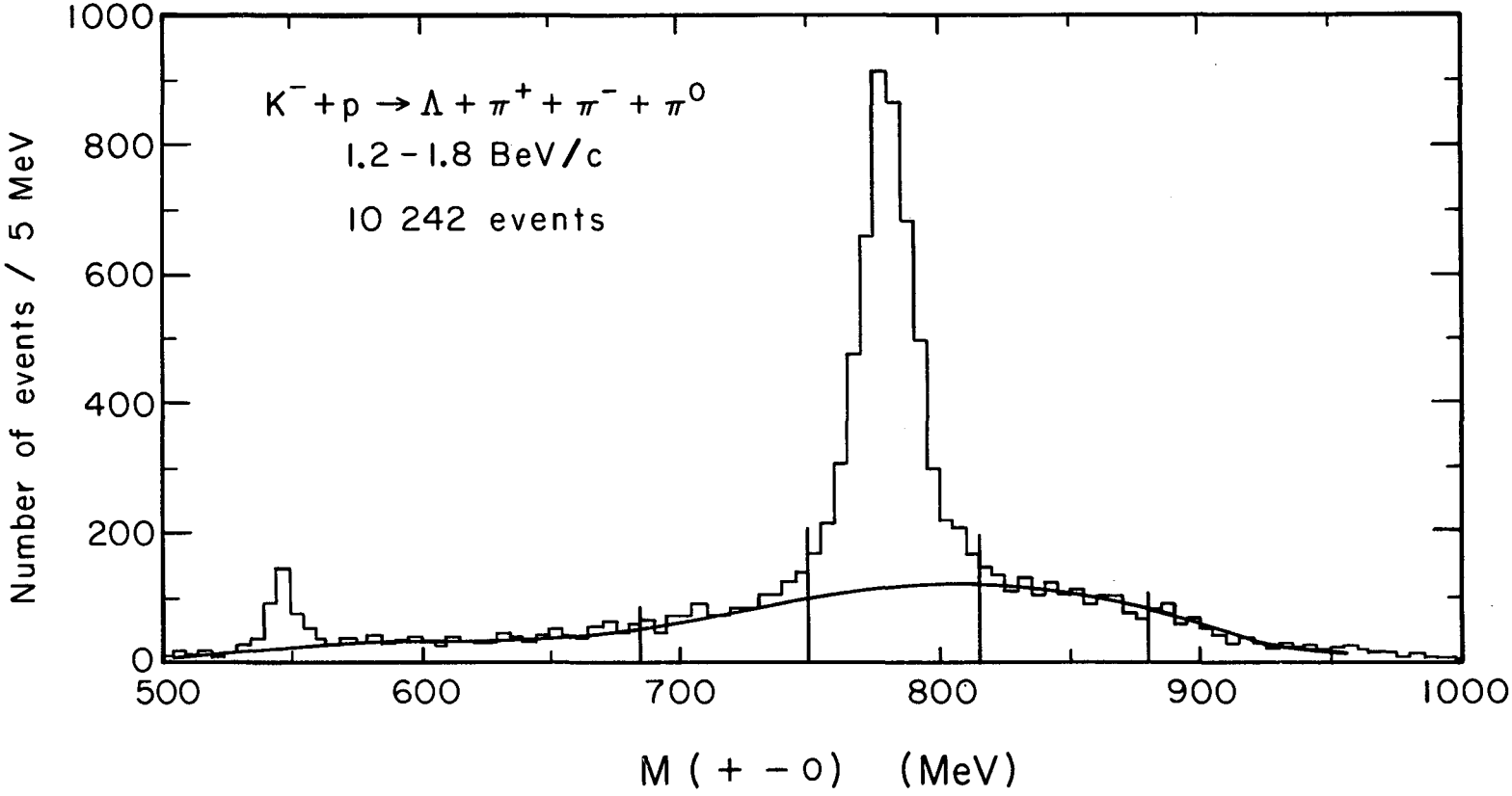

MUB-5812

Fig. 4

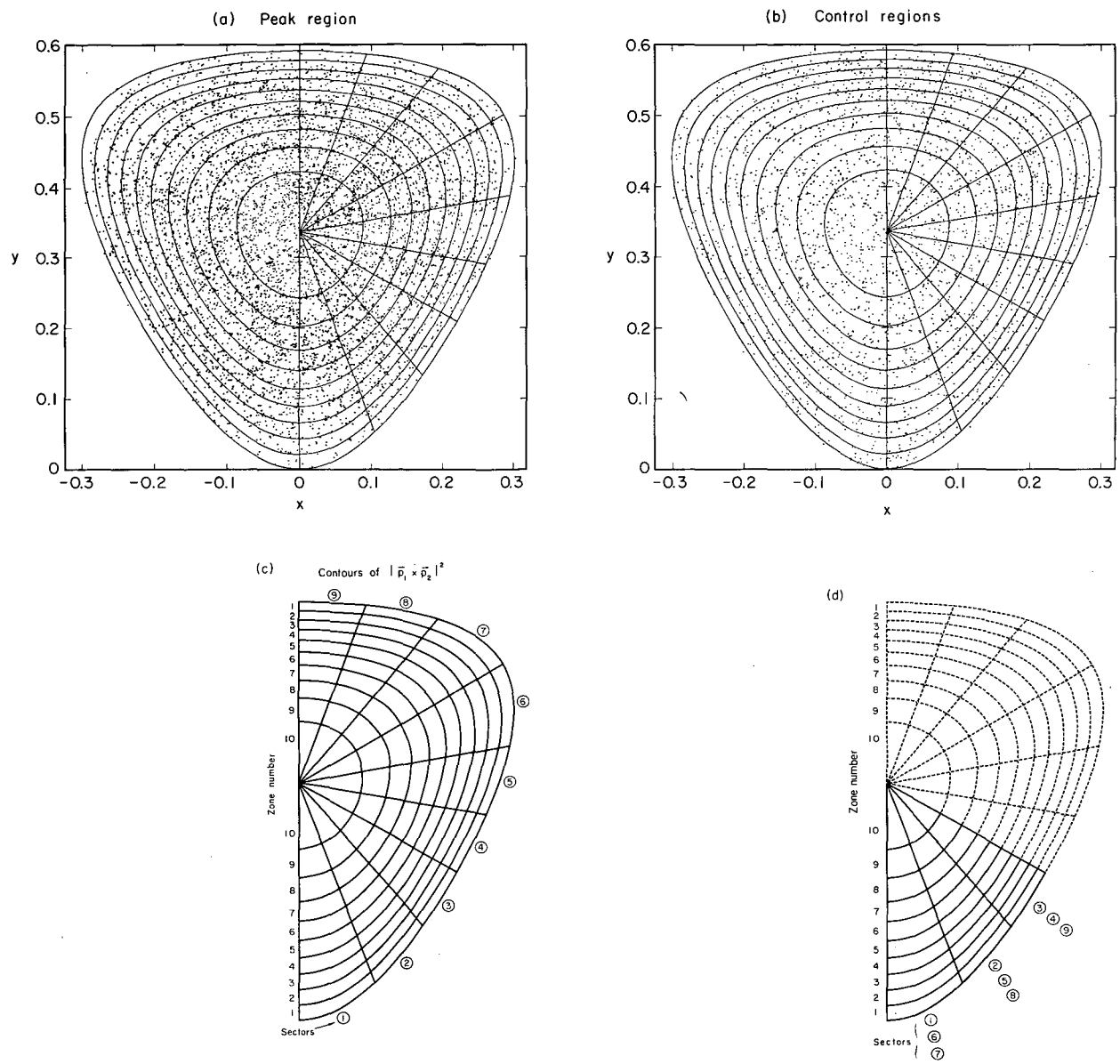

MUB-5850

Fig. 5

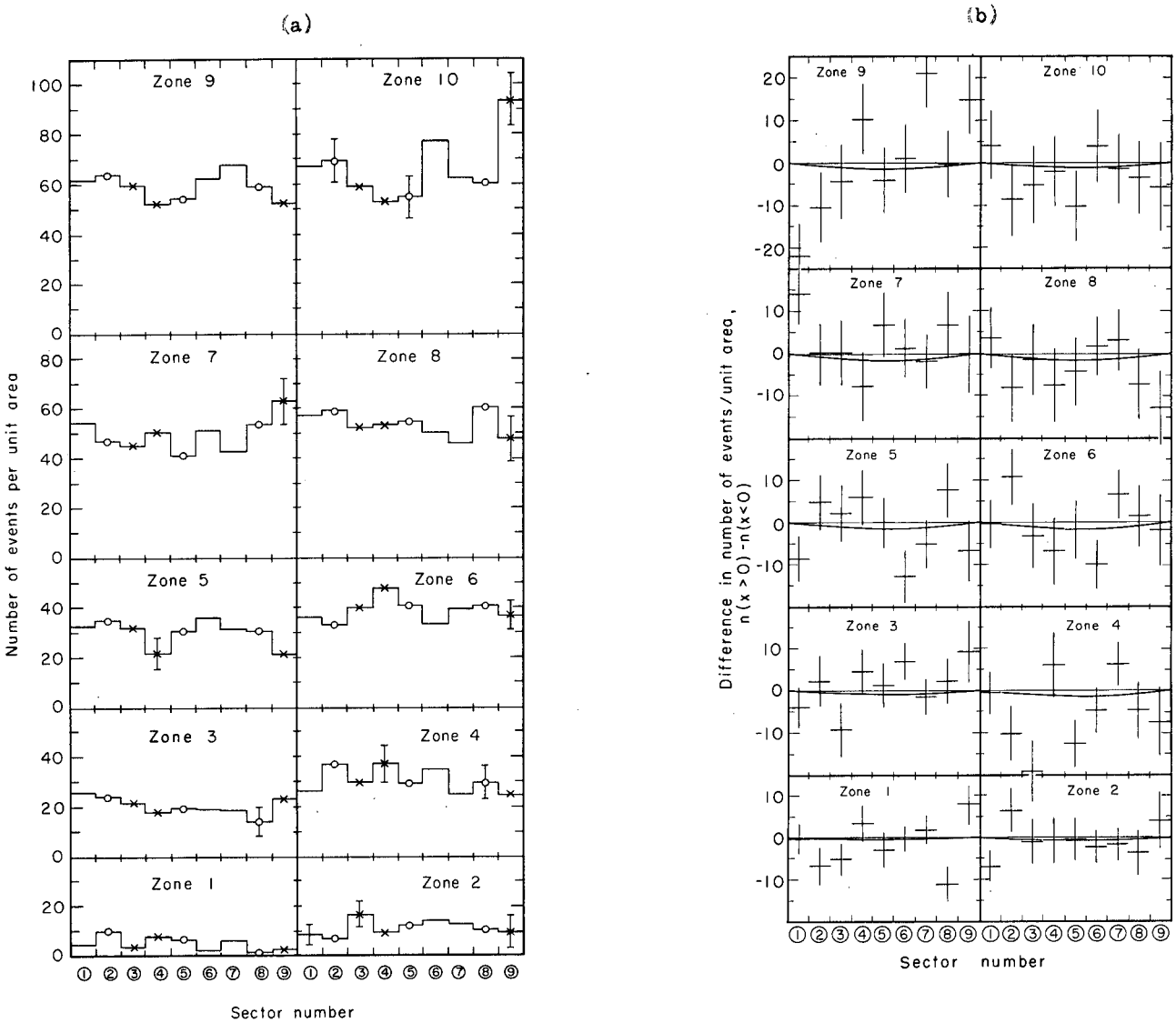

MUB-8313

Fig. 6

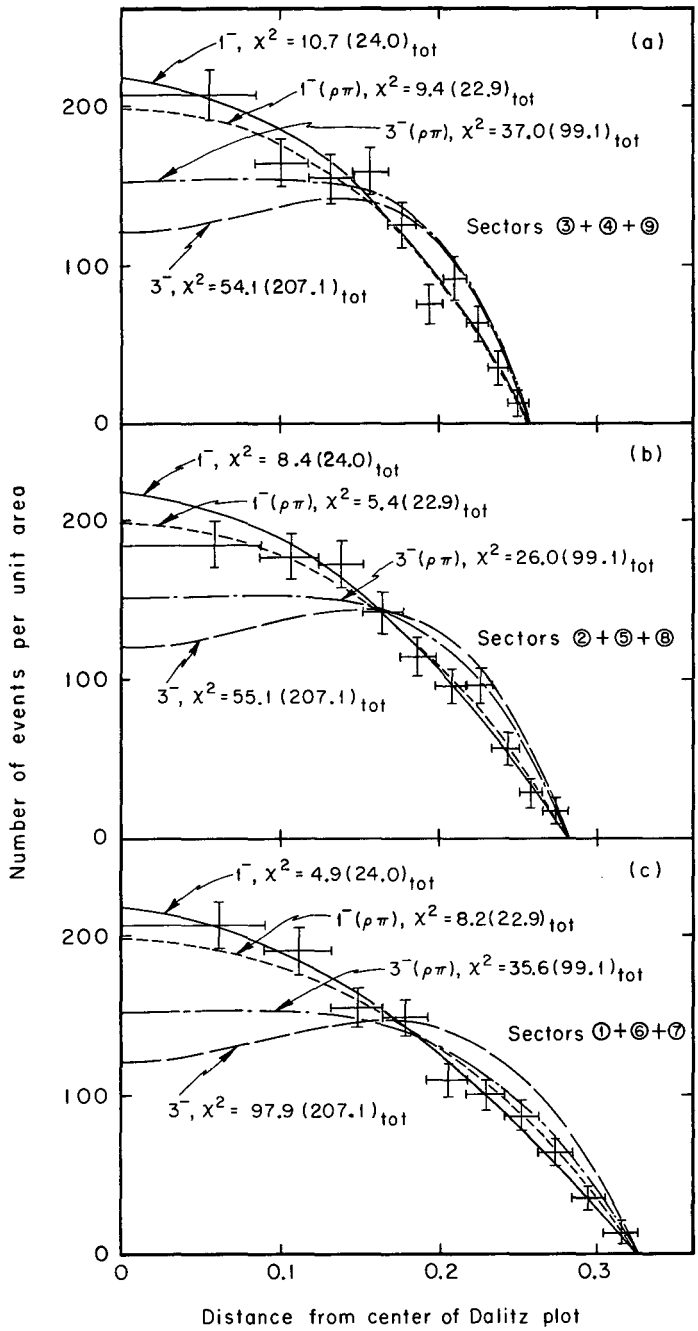

MUB-6581

Fig. 7

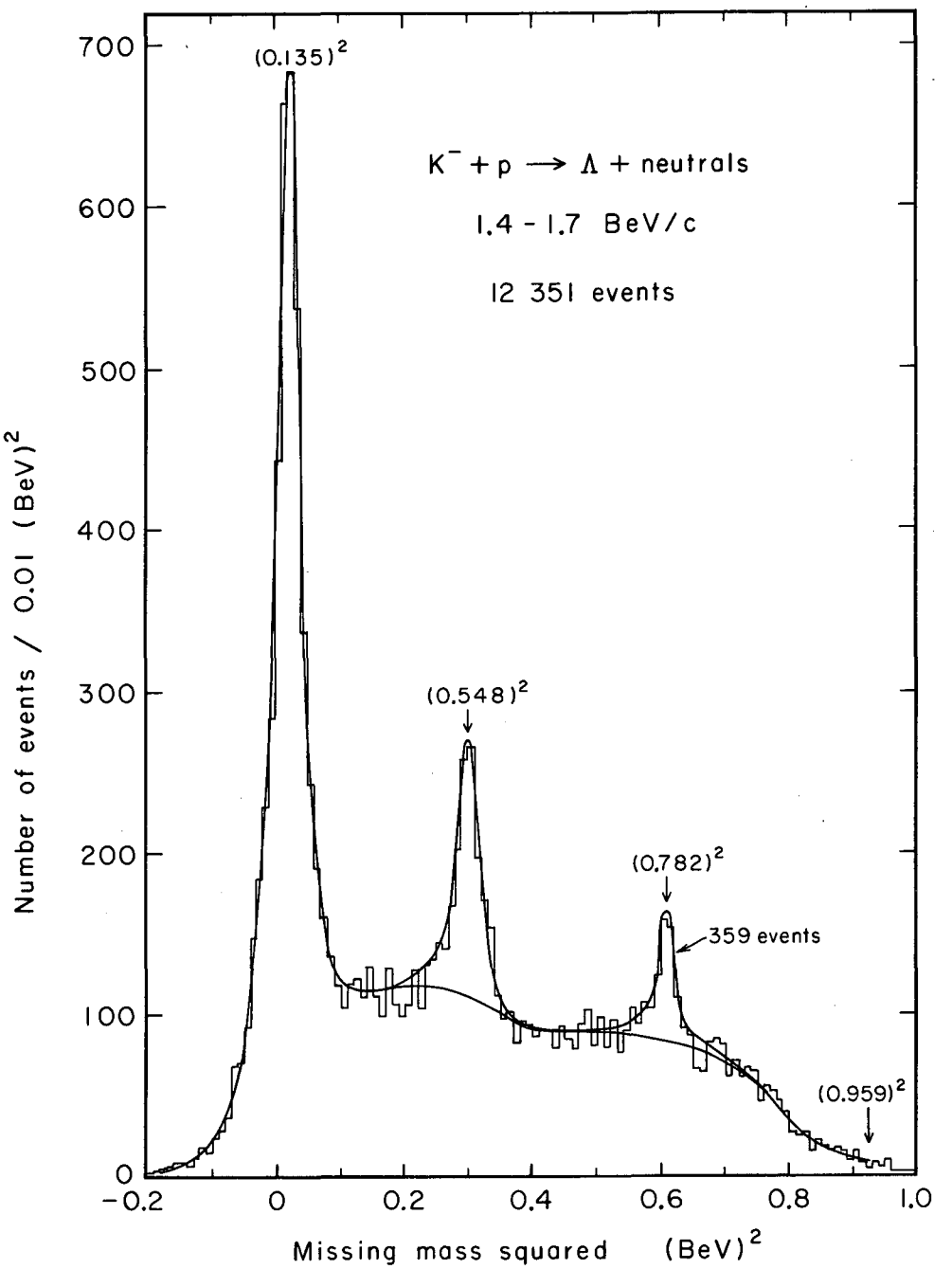

MUB-5814

Fig. 8

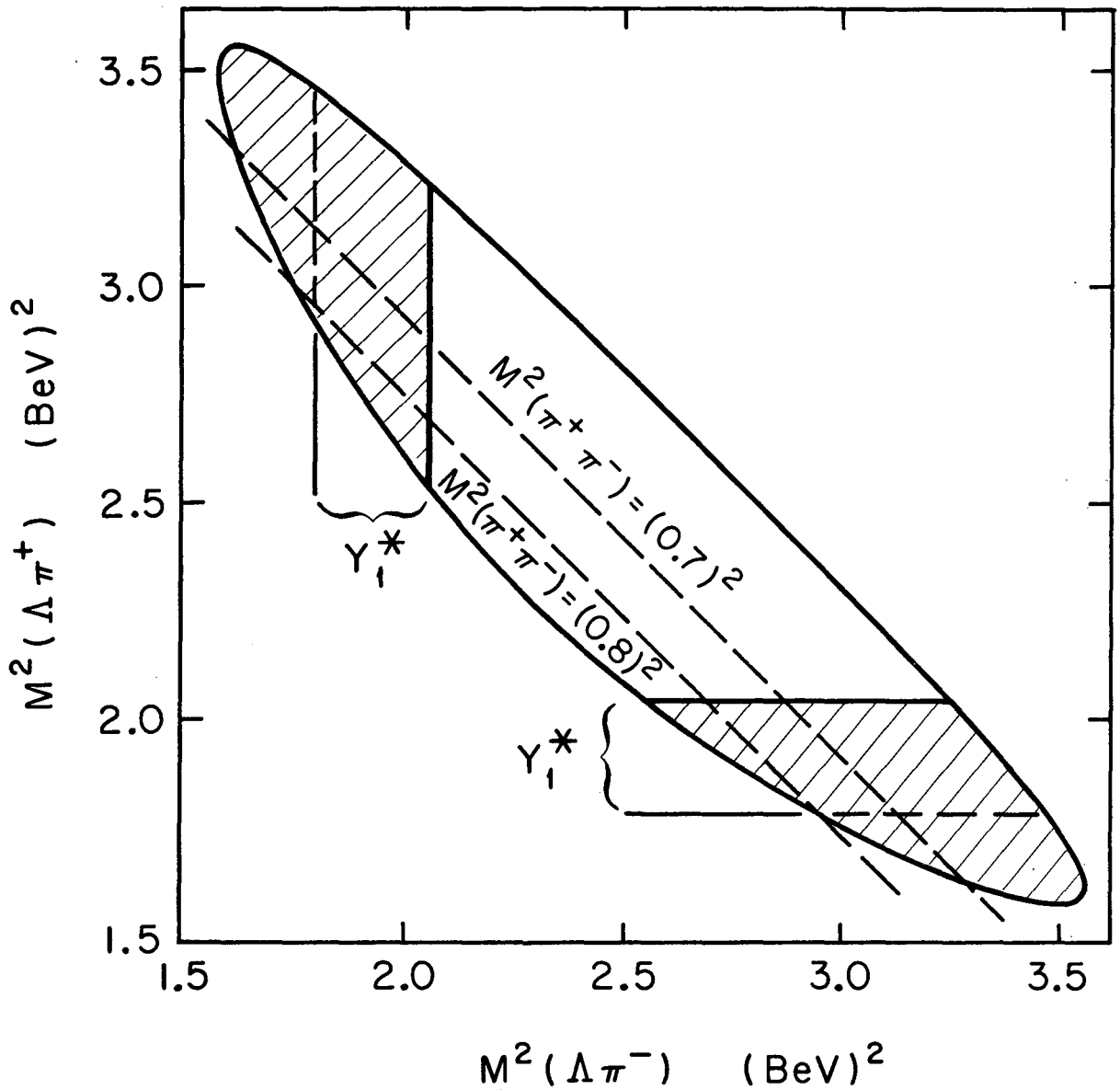

MUB-5750

Fig. 9

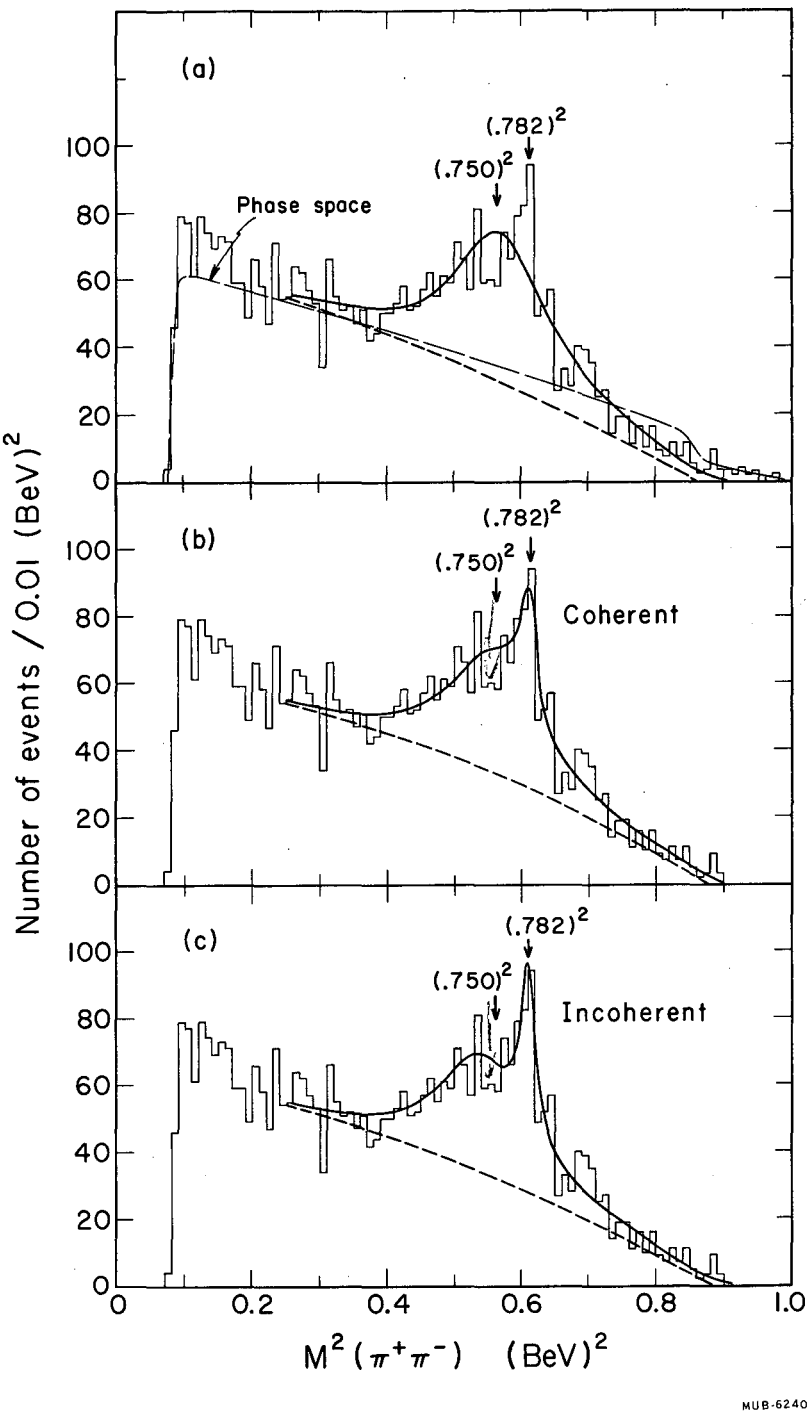
(a)
(.782)^2
(.750)^2
Phase space
(b)
(.782)^2
(.750)^2
Coherent
(c)
(.782)^2
(.750)^2
Incoherent
Number of events / 0.01 (BeV)^2
0
20
40
60
80
100
0
0.2
0.4
0.6
0.8
1.0
$M^2(\pi^+\pi^-)$ (BeV)^2
MUB-6240

Fig. 10

Chi-squared contours
for $\omega \longrightarrow \pi^+ + \pi^-$ amplitude in $K^- + p \rightarrow \Lambda + \omega$
1.2 to 1.7 BeV/c

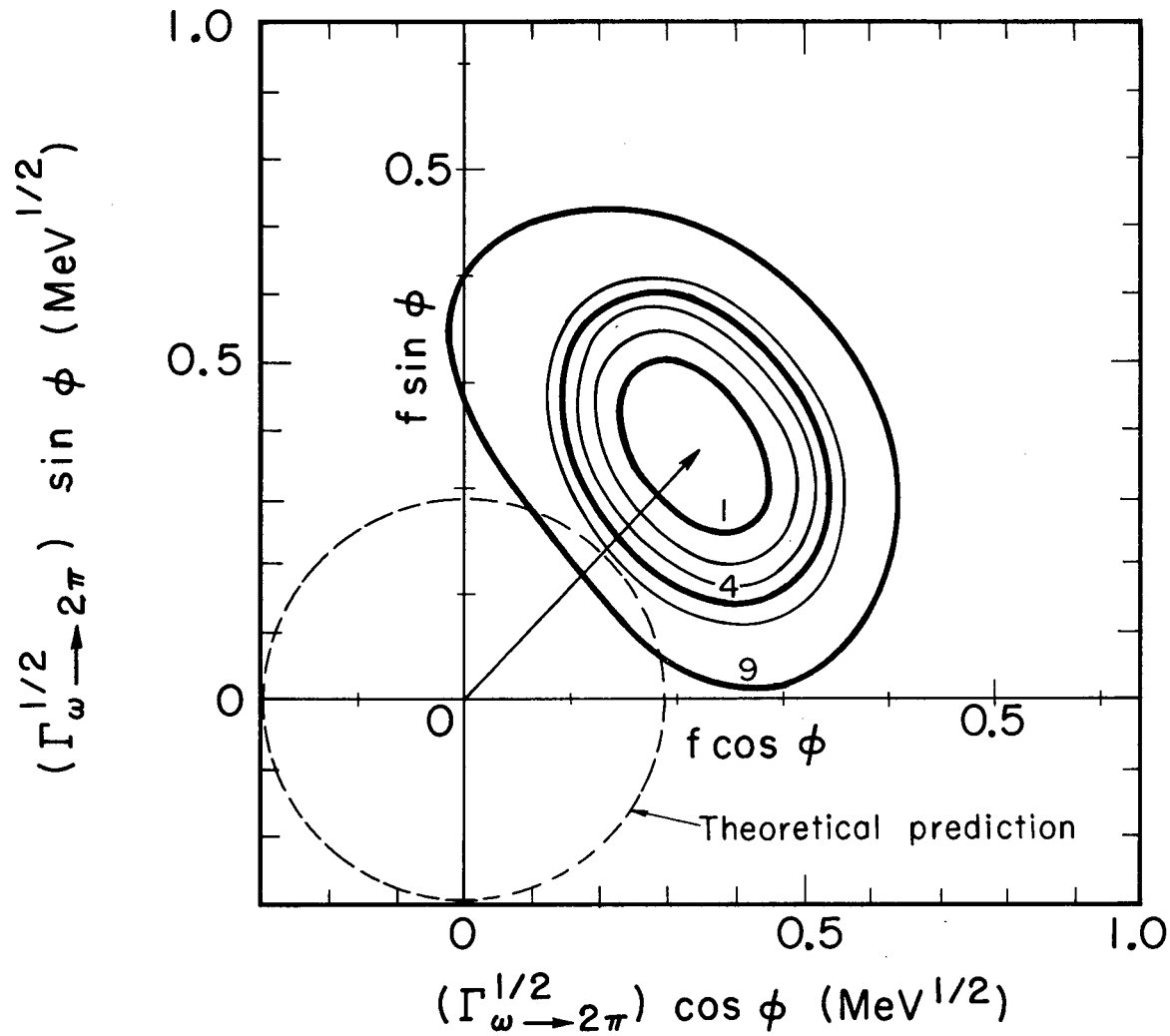

MUB-5820

Fig. 11

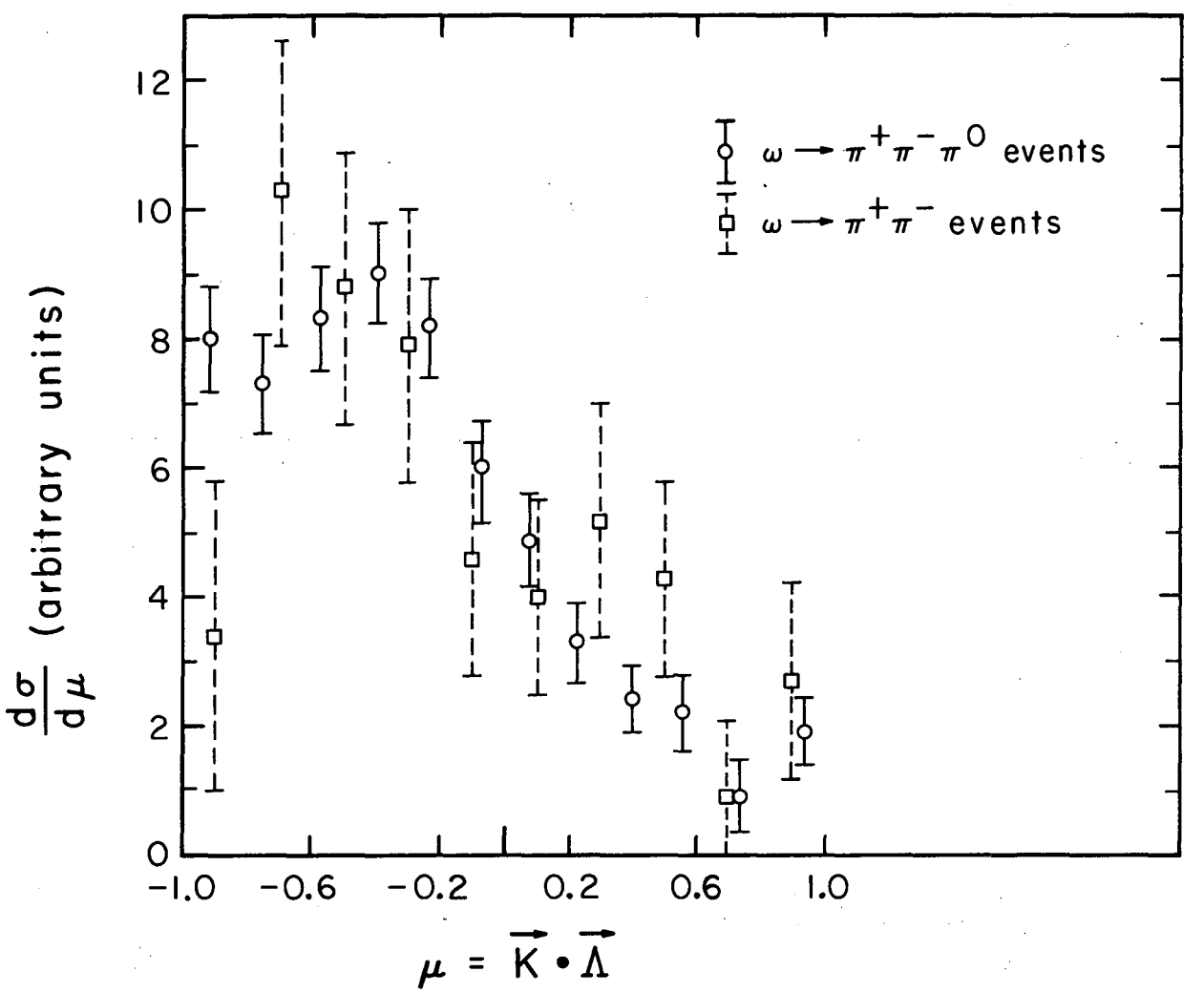

MUB-8386

Fig. 12

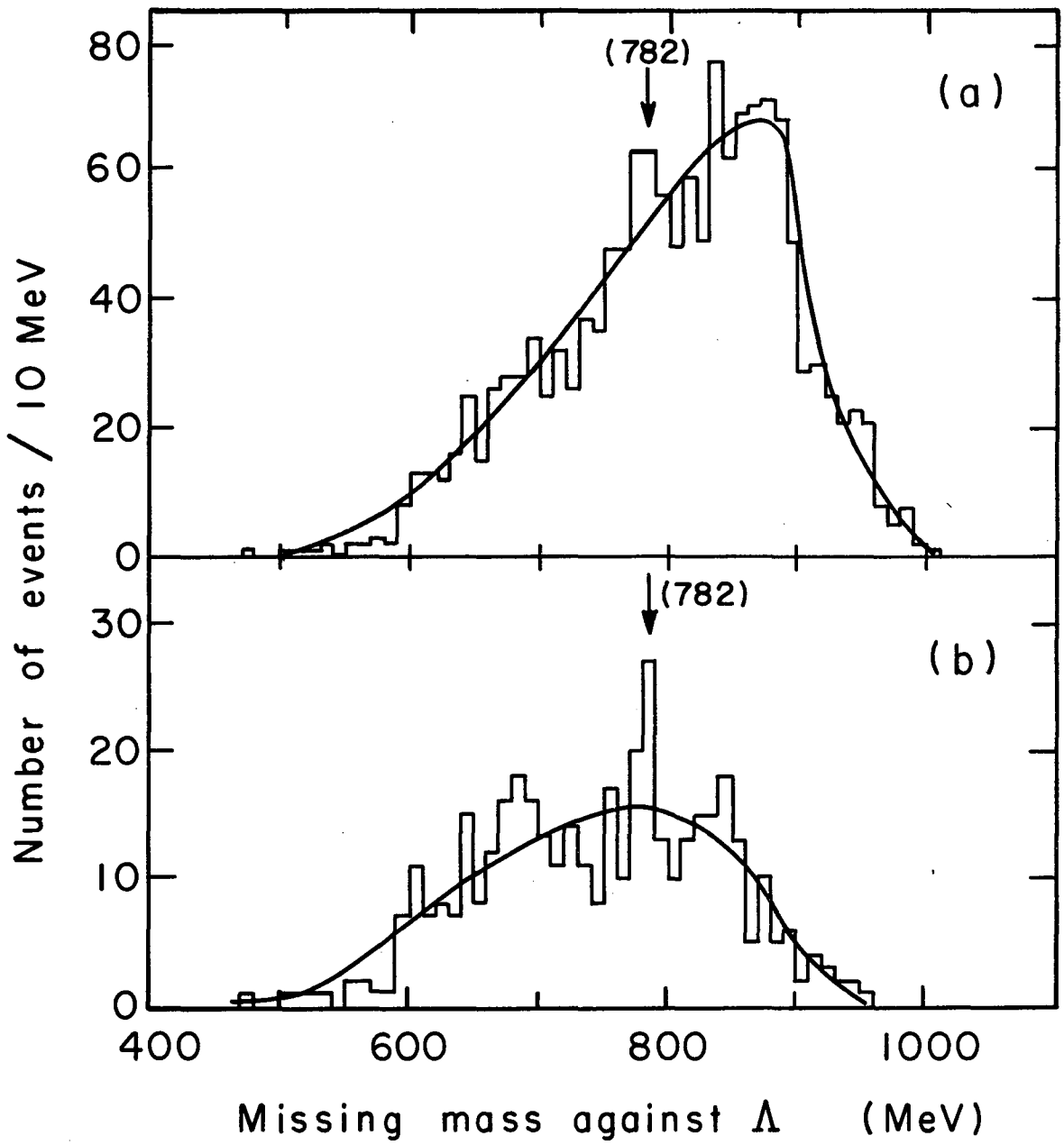

MUB-5805

Fig. 13

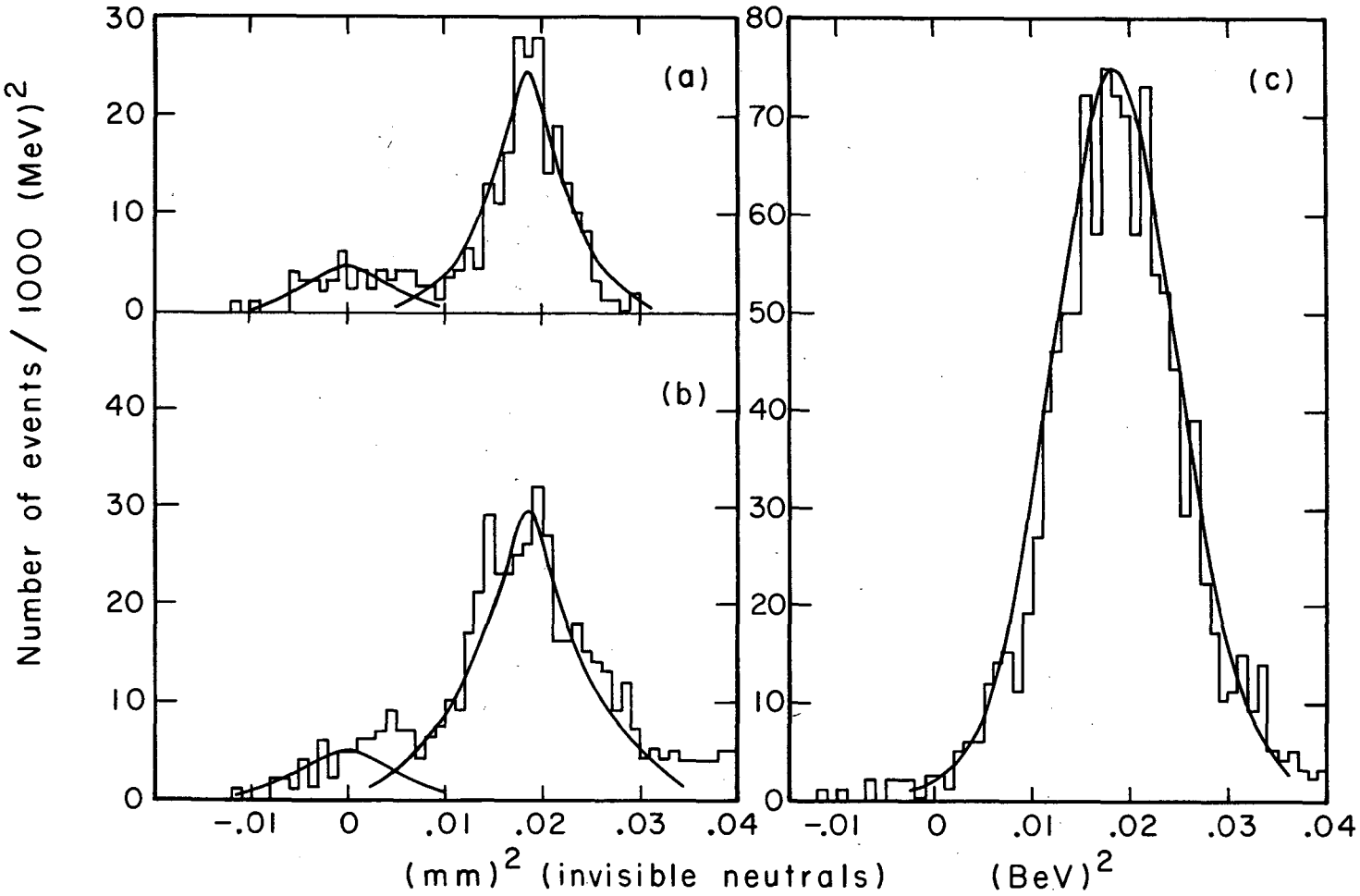

MUB-5810

Fig. 14

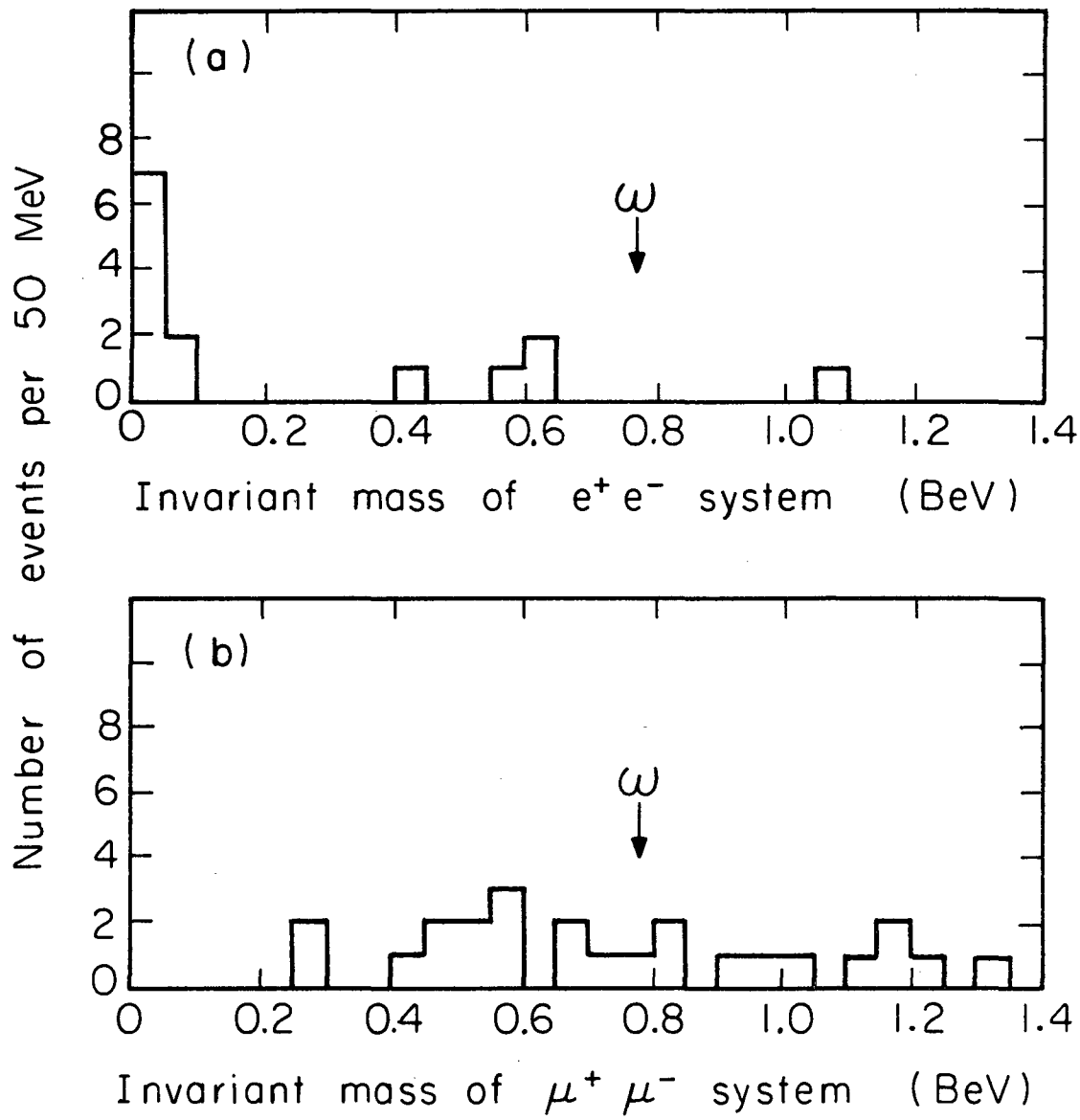
(a)
ω
8
6
4
2
0
0
0.2
0.4
0.6
0.8
1.0
1.2
1.4
Invariant mass of $e^+ e^-$ system (BeV)
Number of events per 50 MeV
(b)
ω
8
6
4
2
0
0
0.2
0.4
0.6
0.8
1.0
1.2
1.4
Invariant mass of $\mu^+ \mu^-$ system (BeV)

MUB-8505

This report was prepared as an account of Government sponsored work. Neither the United States, nor the Commission, nor any person acting on behalf of the Commission:

A. Makes any warranty or representation, expressed or implied, with respect to the accuracy, completeness, or usefulness of the information contained in this report, or that the use of any information, apparatus, method, or process disclosed in this report may not infringe privately owned rights; or

B. Assumes any liabilities with respect to the use of, or for damages resulting from the use of any information, apparatus, method, or process disclosed in this report.

As used in the above, "person acting on behalf of the Commission" includes any employee or contractor of the Commission, or employee of such contractor, to the extent that such employee or contractor of the Commission, or employee of such contractor prepares, disseminates, or provides access to, any information pursuant to his employment or contract with the Commission, or his employment with such contractor.